

# Cardiomyocyte and Myocardial Development

---

### Perspective

Adriana C. Gittenberger-de Groot

The heart is the first crucial functioning organ in a developing embryo. The cell essential for the pumping of the blood through the vascular system is the cardiomyocyte. Cardiomyocyte precursors (CPCs) develop in the mesoderm of the embryo in close association with the endoderm. Recent advances in our knowledge on CPC show that during the initial formation of the heart tube, the so-called first heart field (FHF) progenitors are important. These primarily form the left ventricle of the mature heart. Thereafter, second heart field (SHF) CPCs add the right ventricle and outflow tract as well as part of the inflow tract to the looping heart tube. During the process of addition and looping, septation and valve formation take place. The resultant is a four-chambered heart with a unidirectional flow from the right and left atria to the right and left ventricles and respective pulmonary trunk and ascending aorta. This complex remodeling process is highly dependent on instructive and cellular contribution from various surrounding cell populations. These comprise in the early embryo the endoderm as well as later on the endocardium and the epicardium with its epicardium-derived cells (EPDCs). These cell populations are essential in their interaction with the immature myocardial cells for their proper differentiation and the eventual myocardial architecture. Last but not least, the development of a coronary vascular system with endothelial cells and EPDC-derived smooth muscle cells completes the demands of the oxygenation of the cardiomyocytes. Whether the differentiation of a specific population of the

---

A.C. Gittenberger-de Groot (✉)

Departments Cardiology, Leiden University Medical Center, Leiden, The Netherlands

Anatomy and Embryology, Leiden University Medical Center, Leiden, The Netherlands

e-mail: [A.C.Gittenberger-de\\_Groot@lumc.nl](mailto:A.C.Gittenberger-de_Groot@lumc.nl)

cardiomyocytes into the cardiac conduction system requires an interaction with surrounding cells is still unresolved.

Interest in cardiomyocyte origin and maturation has been highly augmented by the use of cardiac stem cells and inducible progenitor cells (iPCs) for therapeutic aims in life-threatening myocardial pathology and possibly in the future congenital heart disease.

In this section, many aspects of cardiomyocyte (patho-)biology are addressed. For the possible use in the future of CPCs, it is essential to know whether there are differences between FHF- and SHF-derived CPCs as they have their specific contributions to the right and left ventricle with again their specific cardiac failure problems. Single cell transcriptome analysis might be a novel technique to unravel this question. In early development, the inductive role of the endoderm with several important molecular factors like FGFs including the importance of the related thyroid hormone system should be considered with a possible impact on cardiac disease.

Intriguing is the question of cardiomyocyte regeneration capacities in the mature heart not only by reactivation of the dormant CPC population but also by understanding the molecular mechanism underlying the normal cardiomyocyte cell cycle. Cardiomyocyte proliferation is highly active in the prenatal heart and stops postnatally. Understanding of the mechanism underlying this process and the possibility to extend or to reactivate cardiomyocyte proliferation, in which *Meis1* is reported to have a role, might be of great clinical value.

Of similar interest are aspects of formation of the architecture of the myocardial wall consisting of 30 % cardiomyocytes and 70 % cardiac fibroblasts. The myocardial wall develops from a simple two-layered structure into a trabecular layer on the inside and a compact layer on the outside. During development, the relative contributions vary in which the compact layer increases in thickness and the trabecular layer through compaction diminishes. A proper balance of trabecular and compact layer formation seems to be regulated by the Notch pathway-mediated endocardial to myocardial interaction. Disturbance of this pathway in mice may result in a phenotype that resembles a left ventricular non-compaction cardiomyopathy (LVNC) also observed in human familial mutations in this pathway. Likewise, epicardial to myocardial interaction is essential for compact myocardial layer formation as well as ventricular septation. A role of the epicardium in the formation of an anterior-folding ventricular septum is described, shedding new light on the development of ventricular septal defects.

In conclusion, understanding of myocardial pathology and resultant therapeutic and preventive measures, in CHD as well as adult cardiovascular disease, deserves a highly diverse research approach as is elegantly highlighted in this section.

Kenta Yashiro and Ken Suzuki

---

## Abstract

For this decade, heart development has been extensively elucidated by the introduction of the concepts of “heart fields” and “cardiac progenitor cells (CPCs)”. It is believed that multipotent CPCs are specified among the most anterior part of lateral plate mesoderm as belonging to the two anatomical fields; the first heart field (FHF), which is the future left ventricle and atria, and the second heart field (SHF), which is the future right ventricle and outflow tract of the heart. However, the paradigm of two heart fields dependent on conventional marker genes is still disputed, so the existence of independent CPCs specific to each HF remains an open question. In addition, the molecular mechanism underlying the specification of CPCs remains largely unknown. A single-cell transcriptomic approach, which is realized by the recent advances in molecular biology, can be one of the solutions to bring some breakthrough in this subject.

---

## Keywords

Cardiac progenitor cells • First heart field • Second heart field • Single-cell transcriptomics

---

## 10.1 Introduction

Better understanding of the molecular mechanism of heart development is vital to clarify the pathophysiology of congenital heart diseases and will benefit us in terms of prediction, prevention and treatment of such diseases in the future. In addition,

---

K. Yashiro (✉) • K. Suzuki

Translational Medicine and Therapeutics, William Harvey Research Institute, Barts and The London School of Medicine and Dentistry, Queen Mary University of London, Charterhouse Square, London EC1M 6BQ, UK

e-mail: [k.yashiro@qmul.ac.uk](mailto:k.yashiro@qmul.ac.uk)

© The Author(s) 2016

T. Nakanishi et al. (eds.), *Etiology and Morphogenesis of Congenital Heart Disease*,  
DOI 10.1007/978-4-431-54628-3\_10

the information of multipotent cardiac progenitor cells (CPCs) is expected to be valuable for stem cell-based regeneration therapy for the failed heart. However, our knowledge is still insufficient for full translation to the clinical arena.

Here, we review the current knowledge of the earliest phase of cardiac development in mice focusing on CPC specification and discuss the potential of single-cell transcriptomic analyses to elucidate the mechanism [1, 2].

## 10.2 CPCs of the Two Heart Fields

The heart is one of the first anatomical structures formed during embryogenesis. Fate mapping studies indicated that the nascent mesodermal cells contributing to the heart came through the anterior half of primitive streak on embryonic day (E) 6.5 (Fig. 10.1a) [3]. These mesodermal cells migrate anteriorly acquiring the identity of lateral plate mesoderm. At E7.5, the anterior part of lateral plate mesoderm is identified as the heart fields, the direct source of the heart tube [1, 4]. Then the subsequent morphogenesis to create the heart with the four chambers, including the heart tube formation and looping, occurs.

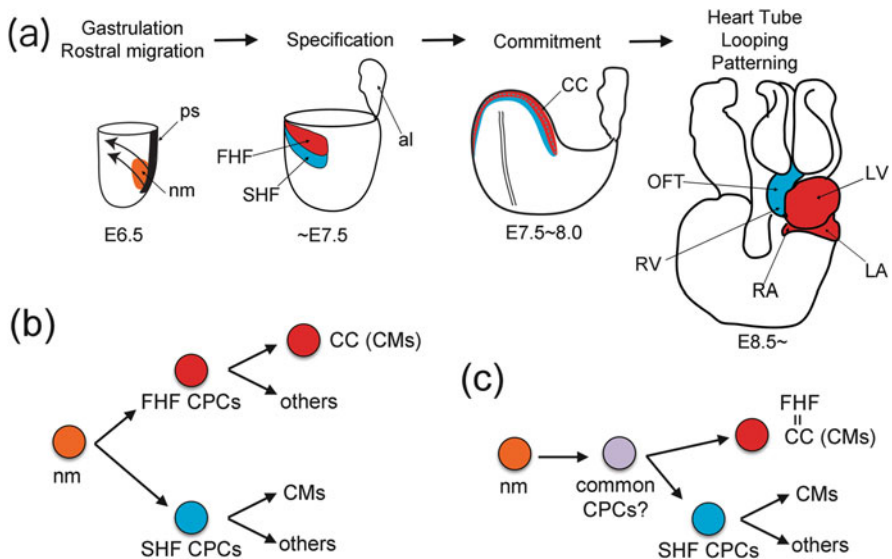


**Fig. 10.1** The heart development. (a) Schematic illustration of the heart development. The progeny of FHF is indicated by *red* and that of SHF is by *blue*. (b) A hypothetical model of the lineage tree of the heart mesoderm. In this model, it is hypothesized that the independent multipotent CPCs of each heart field. (c) An alternative model of the heart mesoderm lineage tree. In this model, common CPCs are hypothesized, and only in the case of SHF, the multipotent state might be maintained. *al* allantois, *CC* cardiac crescent, *CMs* cardiomyocytes, *LA* left atrium, *LV* left ventricle, *nm* nascent mesoderm, *OFT* outflow tract, *ps* primitive streak, *RA* right atrium, *RV* right ventricle

According to the fate map, the anatomical heart fields are divided into two major subgroups, the first heart field (FHF) and the second heart field (SHF) (Fig. 10.1a) [1]. FHF is the classical cardiac crescent and is known to contribute to the left ventricle and parts of the atria. SHF contributes to the right ventricle, outflow tract and also parts of atria. These anatomical fields are currently distinguished with the following molecular markers. The genes encoding transcription factors, *Nkx2-5* and *Tbx5*, mark the FHF, whereas *Isl1* marks the SHF at E7.5 in the mouse [1].

CPCs are believed to appear in the period from gastrulation (E6.5) to the heart fields' formation (E7.5). It is thought that CPCs have been already committed toward the heart but are multipotent to give rise to cardiomyocytes, electric conduction system, smooth muscle and endothelium (Fig. 10.1b, c) [1]. Given the paradigm of the anatomical two heart fields, CPCs are classified into FHF CPCs and SHF CPCs (Fig. 10.1b). Unfortunately multipotent FHF CPCs have not been identified (Fig. 10.1c). The cells in the cardiac crescent, the theoretical progeny of FHF CPCs, are unlikely to be "multipotent progenitors", because these already express the terminal differentiation markers of cardiomyocytes, such as *Actc1* and *Myh7* [1, 5, 6]. To add to this, no marker is available to identify FHF before *Nkx2-5* and *Tbx5* expression. By contrast, the presence of multipotent SHF CPCs, which are marked by *Isl1* expression, seems to be validated with clonal tracing experiments [7]. However, the paradigm of FHF and SHF based on *Nkx2-5* and *Isl1* is now disputed [1]. The expression of *Isl1* was shown to be not specific for SHF and was suggested to represent only the developmental stages [8, 9]. Thus, true characteristics of CPCs should be clarified with revalidation of the conventional biomarkers and the concept of two heart fields.

---

### 10.3 CPC Specification

The molecular mechanism underlying the specification of CPCs remains largely unknown. In the mouse embryo, specification might occur inside the heart fields [1, 4]. When the nascent mesoderm cells at E6.5 containing the presumptive heart fields were transplanted heterotopically to a location other than the heart fields, the fate was not the heart but the same as the cells of the recipient surrounding the graft [4]. On the other hand, when the same graft was transplanted to the heart fields of E7.5, it was committed almost only to the heart. These suggest that the migrating presumptive heart fields are plastic and that some inductive cue for cardiac specification is present within the heart fields. The surrounding tissue, especially the endoderm, likely provides such an inductive cue [1, 4]. However, we cannot exclude the possibility that some sequential events of specification take place during the gastrulation and migration so that the unfixed cardiac competence might be gradually and sequentially consolidated.

It has been shown that the signalling pathways of WNT, FGF, BMP, NODAL (ACTIVIN), SHH and NOTCH are involved in the specification [1, 10]. However, validating the precise role of each signalling pathway is difficult because their

accurate cardiogenic function has been hard to distinguish from their overall effects. Thus, some alternative strategy is needed to bring a breakthrough.

## 10.4 The Potential of Single-Cell Transcriptomics in the Study of CPC Specification

Accurate quantitative evaluation of genome-wide gene expression provides an essential platform to understand the states of cells of interest. In the case where a specific subset of rare cells plays a vital role, single-cell transcriptomics are a strong tool. Indeed, thus far, this strategy has given fruitful results in the study of the specification of the olfactory receptors, spinal cord neurons and primordial germ cells [11–13]. Currently, several protocols of single-cell transcriptomics have been developed as applicable to next-generation sequencing (NGS) with sufficient coverage, sensitivity and accuracy (Table. 10.1) [2].

The protocol for genome-wide analysis was first developed by Kurimoto and colleagues for microarray and has been recently modified for NGS (Fig. 10.2a) [14–16]. The feature of this protocol is to add artificially a poly A tail to the 3'-end of the first-strand cDNA to generate the appropriate adapter sites for PCR amplification. At the final step, cDNA is obtained as PCR amplicon. Disadvantageously Kurimoto's protocol provides only strongly 3'-biased cDNA, although Tang's protocol likely overcomes this problem [15].

Quartz-seq is also a method applicable to microarray and NGS, based on PCR amplification, and the architecture of the protocol is based on "suppressive PCR" (Fig. 10.2a) [17]. This method looks superior to Kurimoto's in terms of simple operation, coverage and technical reproducibility.

SMART-seq utilizes a unique nature of reverse transcriptase [18]. During reverse transcription, Moloney murine leukaemia virus reverse transcriptase adds a short poly C tail to the 3'-end of the first-strand cDNA. Reverse transcriptase uses a helper oligonucleotide with poly G motif as the template ("template switch") after annealing to the poly C tail, which results in the addition of adaptors to cDNA (Fig. 10.2b). This template switch happens preferentially to 5'-capped mRNA so that finally a full-length cDNA library is obtained as suppressive PCR amplicon if oligo(dT) primer is used for the first-strand synthesis. This enrichment of full length

**Table 10.1** Methods of single-cell transcriptomics

Method	Principle	Application	References
Kurimoto et al. 2006	Poly A tailing/PCR	Microarray	[14]
Tang et al. 2009	Poly A tailing/PCR	NGS	[15]
Brouillette et al. 2012	Poly A tailing/PCR	NGS	[16]
Quartz-seq/-chip	Poly A tailing/suppressive PCR	NGS/microarray	[17]
SMART-seq	Template switch/PCR	NGS	[18]
CEL-seq	IVT/PCR	NGS	[19]

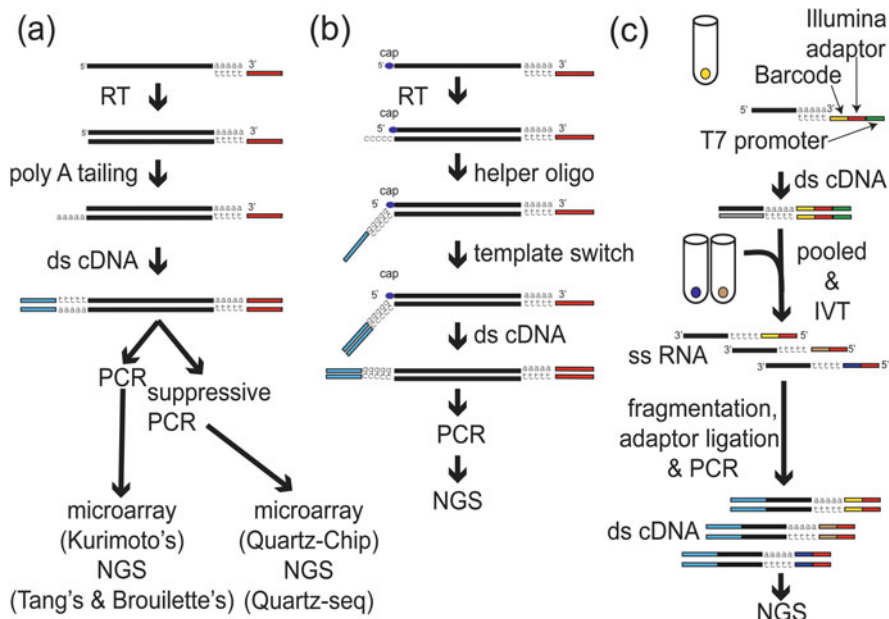


**Fig. 10.2** Overview of the methods of single-cell transcriptomics. (a) Poly A tailing (Kurimoto's, Tang's, Boulette's protocol and Quartz-seq), (b) SMART-seq, (c) CEL-seq. Please refer to the main text and the relevant references for details

is a merit, but simultaneously a demerit, because any partially synthesized cDNAs are not amplified so that the yield of cDNAs is inevitably limited.

On the other hand, CEL-seq uses mainly isothermal amplification of *in vitro* transcription (IVT) by T7 polymerase (Fig. 10.2c) [19]. Theoretically, IVT is superior to PCR in terms of linear and proportional amplification to secure better technical reproducibility. A demerit of this protocol is that reads by NGS are strongly biased toward 3'-end.

Lastly, we should discuss the limitations of single-cell transcriptomics. First, there is always a technical noise due to pipetting error, difference of system (including enzymes, thermal cycler and NGS machine) and amplification bias. Of note, the "Monte Carlo effect", the cause of large quantitative errors of small copy number mRNAs due to the stochastic events within an initial few cycles of PCR reaction, is uncontrollable. Amplification bias is inevitable to some extent in the protocols dependent on PCR, although every protocol has been well validated to secure its sufficient technical reproducibility. Second, the lack of topological information precludes us from referring the obtained expression profile to the cell in the embryo if no molecular markers exist. Thus it is necessary to consider how to fill such lost information.

## 10.5 Future Direction and Clinical Implication

The strategy of single-cell transcriptomics has great potential to increase understanding of CPC specification, their ground state and differentiation. This knowledge will be utilized in order to control the commitment of pluripotent stem cells including ES cells and iPS cells for future clinical application as stem cell-based regeneration therapy.

**Acknowledgements** We thank Kazuko Koshiba-Takeuchi, Jun Takeuchi, Shigetoyo Kogaki, Manabu Shirai, Hiroki Kokubo, Yusuke Watanabe and Hiroyuki Yamagishi for helpful discussions and Steven Coppen for editing. Our work is supported by MRC New Investigator Research Grant G0900105, MRC Research Grant MR/J007625/1 and BHF Project Grant PG/11/102/29213 to KY.

**Open Access** This chapter is distributed under the terms of the Creative Commons Attribution-Noncommercial 2.5 License (<http://creativecommons.org/licenses/by-nc/2.5/>) which permits any noncommercial use, distribution, and reproduction in any medium, provided the original author(s) and source are credited.

The images or other third party material in this chapter are included in the work's Creative Commons license, unless indicated otherwise in the credit line; if such material is not included in the work's Creative Commons license and the respective action is not permitted by statutory regulation, users will need to obtain permission from the license holder to duplicate, adapt or reproduce the material.

---

## References

1. Rana MS, Christoffels VM, Moorman AF. A molecular and genetic outline of cardiac morphogenesis. *Acta Physiol (Oxf)*. 2013;207:588–615.
2. Shapiro E, Biezuner T, Linnarsson S. Single-cell sequencing-based technologies will revolutionize whole-organism science. *Nat Rev Genet*. 2013;14:618–30.
3. Kinder SJ, Tsang TE, Quinlan GA, et al. The orderly allocation of mesodermal cells to the extraembryonic structures and the anteroposterior axis during gastrulation of the mouse embryo. *Development*. 1999;126:4691–701.
4. Tam PP, Parameswaran M, Kinder SJ, et al. The allocation of epiblast cells to the embryonic heart and other mesodermal lineages: the role of ingression and tissue movement during gastrulation. *Development*. 1997;124:1631–42.
5. Takeuchi JK, Bruneau BG. Directed transdifferentiation of mouse mesoderm to heart tissue by defined factors. *Nature*. 2009;459:708–11.
6. Cai CL, Liang X, Shi Y, et al. *Isl1* identifies a cardiac progenitor population that proliferates prior to differentiation and contributes a majority of cells to the heart. *Dev Cell*. 2003;5:877–89.
7. Moretti A, Caron L, Nakano A, et al. Multipotent embryonic *isl1*+ progenitor cells lead to cardiac, smooth muscle, and endothelial cell diversification. *Cell*. 2006;127:1151–65.
8. Prall OW, Menon MK, Solloway MJ, et al. An *Nkx2-5/Bmp2/Smad1* negative feedback loop controls heart progenitor specification and proliferation. *Cell*. 2007;128:947–59.
9. Ma Q, Zhou B, Pu WT. Reassessment of *Isl1* and *Nkx2-5* cardiac fate maps using a *Gata4*-based reporter of *Cre* activity. *Dev Biol*. 2008;323:98–104.
10. Nemir M, Croquelois A, Pedrazzini T, et al. Induction of cardiogenesis in embryonic stem cells via downregulation of *Notch1* signaling. *Circ Res*. 2006;98:1471–8.



11. Dulac C, Axel R. A novel family of genes encoding putative pheromone receptors in mammals. *Cell*. 1995;83:195–206.
12. Tanabe Y, William C, Jessell TM. Specification of motor neuron identity by the MNR2 homeodomain protein. *Cell*. 1998;95:67–80.
13. Saitou M, Barton SC, Surani MA. A molecular programme for the specification of germ cell fate in mice. *Nature*. 2002;418:293–300.
14. Kurimoto K, Yabuta Y, Ohinata Y, et al. An improved single-cell cDNA amplification method for efficient high-density oligonucleotide microarray analysis. *Nucleic Acids Res*. 2006;34:e42.
15. Tang F, Barbacioru C, Wang Y, et al. mRNA-Seq whole-transcriptome analysis of a single cell. *Nat Methods*. 2009;6:377–82.
16. Brouillette S, Kuersten S, Mein C, et al. A simple and novel method for RNA-seq library preparation of single cell cDNA analysis by hyperactive Tn5 transposase. *Dev Dyn*. 2012;241:1584–90.
17. Sasagawa Y, Nikaido I, Hayashi T, et al. Quartz-Seq: a highly reproducible and sensitive single-cell RNA sequencing method, reveals non-genetic gene-expression heterogeneity. *Genome Biol*. 2013;14:R31.
18. Ramskold D, Luo S, Wang YC, et al. Full-length mRNA-Seq from single-cell levels of RNA and individual circulating tumor cells. *Nat Biotechnol*. 2012;30:777–82.
19. Hashimshony T, Wagner F, Sher N, et al. CEL-Seq: single-cell RNA-Seq by multiplexed linear amplification. *Cell Rep*. 2012;2:666–73.

---

# Meis1 Regulates Postnatal Cardiomyocyte Cell Cycle Arrest

# 11

Shalini A. Muralidhar and Hesham A. Sadek

---

## Abstract

The neonatal mammalian heart is capable of substantial regeneration following injury through cardiomyocyte proliferation (Porrello et al, *Science* 331:1078–1080, 2011; *Proc Natl Acad Sci U S A* 110:187–92, 2013). However, this regenerative capacity is lost by postnatal day 7 and the mechanisms of cardiomyocyte cell cycle arrest remain unclear. The homeodomain transcription factor Meis1 is required for normal cardiac development but its role in cardiomyocytes is unknown (Paige et al, *Cell* 151:221–232, 2012; Wamstad et al, *Cell* 151: 206–220, 2012). Here we identify Meis1 as a critical regulator of the cardiomyocyte cell cycle. Meis1 deletion in mouse cardiomyocytes was sufficient for extension of the postnatal proliferative window of cardiomyocytes and for reactivation of cardiomyocyte mitosis in the adult heart with no deleterious effect on cardiac function. In contrast, overexpression of Meis1 in cardiomyocytes decreased neonatal myocyte proliferation and inhibited neonatal heart regeneration. Finally, we show that Meis1 is required for transcriptional activation of the synergistic CDK inhibitors p15, p16, and p21. These results identify Meis1 as a critical transcriptional regulator of cardiomyocyte proliferation and a potential therapeutic target for heart regeneration.

---

## Keywords

Cardiomyocytes • Heart injury • Regeneration • Meis1 • Cell cycle

---

S.A. Muralidhar, Ph.D. • H.A. Sadek, M.D., Ph.D. (✉)

Department of Internal Medicine, Division of Cardiology, The University of Texas Southwestern Medical Center, Dallas, TX 75390, USA

e-mail: [hesham.sadek@utsouthwestern.edu](mailto:hesham.sadek@utsouthwestern.edu)

© The Author(s) 2016

T. Nakanishi et al. (eds.), *Etiology and Morphogenesis of Congenital Heart Disease*, DOI 10.1007/978-4-431-54628-3\_11

93

## 11.1 Introduction

The past decade witnessed a revolution in our understanding of cardiac biology, with groundbreaking research demonstrating that the adult mammalian heart is capable of limited but measurable cardiomyocyte turnover [5–9]. However, the ultimate goal of complete regeneration of the heart remains elusive. In stark contrast to the adult mammalian heart, we recently demonstrate that the mammalian heart is in fact capable of complete regeneration following apical resection of 15 % of the ventricular myocardium [1]. This remarkable regenerative capacity was associated with robust cardiomyocyte proliferation throughout the myocardium. Moreover, lineage-tracing studies demonstrated that the newly formed myocytes were derived from preexisting cardiomyocytes, rather than from a progenitor population. Finally, we showed that cessation of this regenerative phenomenon occurred at postnatal day 7 (P7), which coincides with the developmental window when cardiomyocytes become binucleate and withdraw from the cell cycle [9, 10]. It is unclear whether the loss of this regenerative potential in the adult heart is due to an intrinsic cell cycle block in adult cardiomyocytes or to loss of mitogenic stimuli as the heart ages (or both). Thus, it is important to determine the mechanisms by which the mammalian heart switches off this regenerative capacity in the week after birth.

In an effort to identify genes involved in postnatal regeneration arrest, we performed several gene arrays following MI at multiple postnatal time points. This allowed us to identify *Meis1* as one of the few transcription factors that were dysregulated between injury at P1 and injury at P7 and P14. *Meis1* has been studied extensively in the hematopoietic system, is required for normal hematopoiesis, and also plays an important role in leukemogenic transformation [11–14]. What little is known about the role of *Meis1* in the heart comes from global KO studies resulting in numerous cardiac defects. However, given that global *Meis1* deletion results in embryonic lethality by E14.5, full characterization of the role of *Meis1* in cardiomyocytes has been difficult [13, 15, 16]. Despite the role of *Meis1* in regulation of hematopoiesis and cardiac development, the mechanism of action of *Meis1* remains poorly characterized. Our results indicate that *Meis1* expression and nuclear localization in cardiomyocytes coincide with cell cycle arrest. Cardiomyocyte cell cycle exit is associated with downregulation of positive cell cycle regulators (CDK2, CDK3, CDK4, CCND1, and CDK cofactors) and induction of cell cycle inhibitors (CDKI, members of the INK4 and CIP/KIP families) [10, 17–20]. We identified conserved *Meis1* domains in only two key CDK inhibitors, namely, p16 and p21, which are known to regulate all three cell cycle checkpoints. We demonstrated that *Meis1* regulates the pattern of expression of these two cell cycle inhibitors following *Meis1* knockdown. These results provide role and mechanism of cell cycle regulation by *Meis1*.

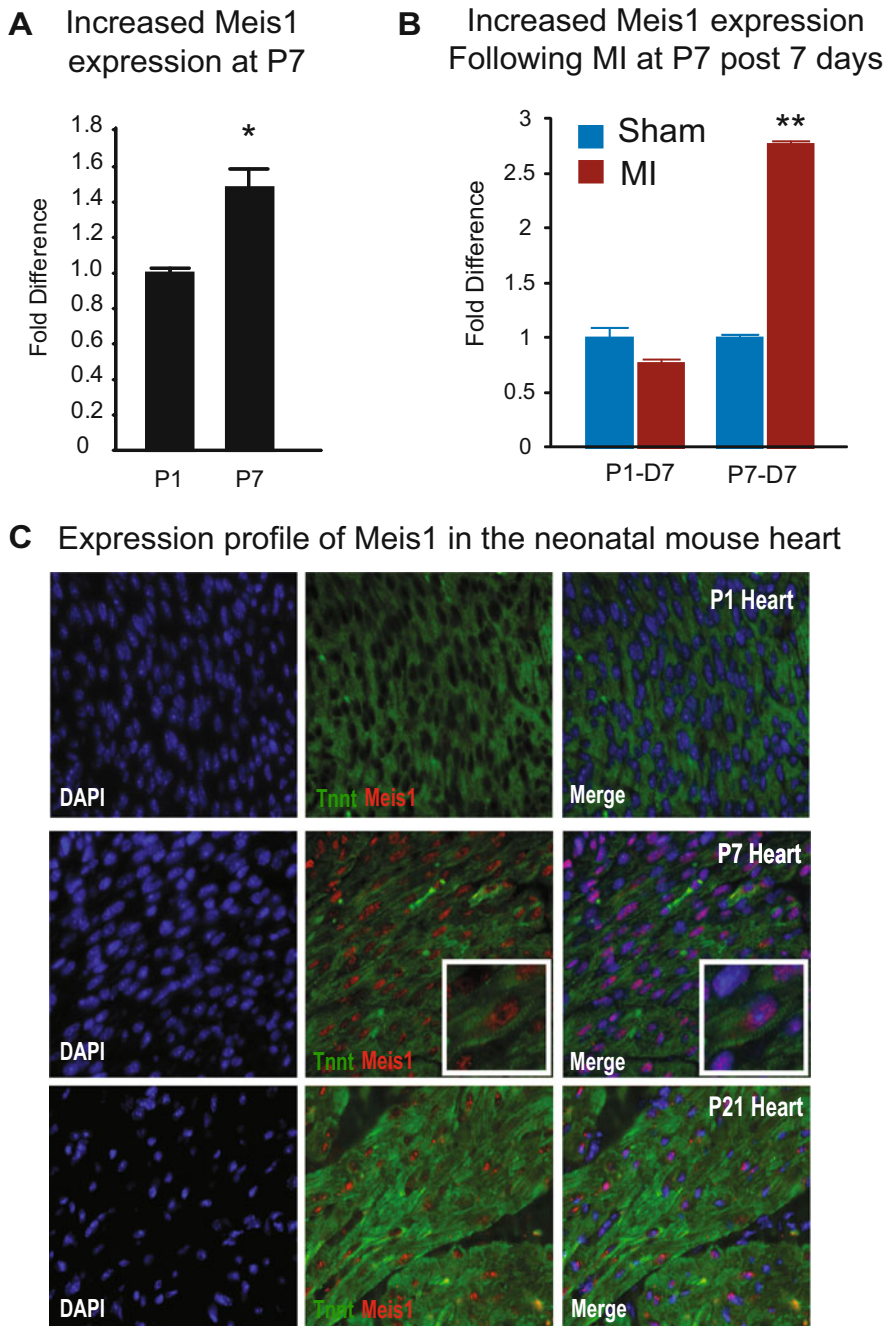


**Fig. 11.1** Expression profile of Meis1 in postnatal heart. (a) qRT-PCR showing increased expression of Meis1 at postnatal day 7 (P7), a time point that coincides with cell cycle arrest of cardiomyocytes. (b) qRT-PCR showing expression levels of Meis1 7 days post Sham or MI at P1 or P7. (c) Expression of Meis1 is absent at P1 and nuclear localization of Meis1 in P7 and P21 cardiomyocytes

## 11.2 Results

### 11.2.1 Expression of Meis1 During Neonatal Heart Development and Regeneration

Transcriptional regulation of postnatal cardiomyocyte cell cycle arrest is unclear. Our initial screens identified Meis1 as a potential transcriptional regulator of neonatal heart regeneration. Therefore, we conducted this study to determine the role of Meis1 in regulation of cardiomyocyte cell cycle. We first examined the expression pattern of Meis1 during neonatal heart development and regeneration. qPCR showed a modest increase in Meis1 expression between postnatal day 1 (P1) and P7 (Fig. 11.1a). Meis1 was localized to perinuclear regions in neonatal cardiomyocytes at P1 and nuclear localized by P7 and P21 (Fig. 11.1c). Myocardial infarction (MI) at P1, which is associated with an induction of robust cardiomyocyte proliferation at day 7 post-MI, was associated with a modest decrease in the expression of Meis1, whereas Meis1 mRNA expression levels were significantly increased following MI at P7, a time point coinciding with lack of mitotic induction of cardiomyocytes (Fig. 11.1b).

### 11.2.2 Cardiomyocyte Proliferation Beyond Postnatal Day 7 Following Meis1 Deletion

We generated cardiomyocyte-specific Meis1 knockout (KO) mice by crossing Meis1<sup>fl/fl</sup> mice with  $\alpha$ MHC-Cre mice (Fig. 11.2a). qRT-PCR of cardiomyocytes from Meis1<sup>fl/fl</sup>  $\alpha$ MHC-Cre (Meis1KO) compared to  $\alpha$ MHC-Cre (control) mouse hearts confirmed a change in gene expression consistent with Meis1 deletion in cardiomyocytes (Fig. 11.2b). Phenotypic characterization of Meis1KO mice at P14 (1 week beyond the normal window of postnatal cardiomyocyte cell cycle arrest) demonstrated that heart size (Fig. 11.2c, d) and cardiac function (Fig. 11.2e) were unaffected by Meis1 deletion. However, Meis1KO cardiomyocytes were smaller compared to control cardiomyocytes (Fig. 11.2f), which may imply that the cardiomyocyte number is increased in Meis1KO (smaller cardiomyocyte size, with no change in heart-to-body weight ratio). Therefore, we examined the Meis1KO hearts for myocyte proliferation using the mitosis marker pH3 (phosphorylated histone H3) and the cytokinesis marker Aurora B kinase. Meis1 deletion resulted in induction of cardiomyocyte proliferation as quantified by an increase in the number of pH3+TnnT2+ (troponin T2) cells (Fig. 11.2g). In addition, we found that Aurora B was markedly expressed in the cleavage furrow between proliferating myocytes in the KO hearts (0.5-fold) (Fig. 11.2h). We also found a significant increase which did not result in an increase in myocyte apoptosis by TdT-mediated dUTP nick end labeling (TUNEL) staining (Fig. 11.2k).

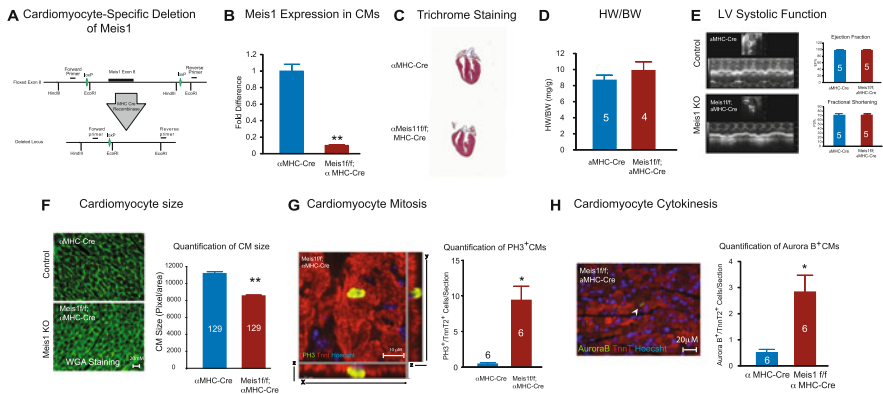


**Fig. 11.2** Cardiomyocyte proliferation at P14 following Meis1 deletion. (a) Schematic of Meis1 floxed allele. Control mice were  $\alpha$ MHC-Cre, Meis1KO mice were Meis1<sup>fl/fl</sup> $\alpha$ MHC-Cre. (b) qRT-PCR demonstrates deletion of Meis1 in cardiomyocytes at P14. (c) Trichrome staining of wild-type (WT) and Meis1KO hearts at P14. (d) Heart weight (HW)-to-body weight (BW) ratio in WT and Meis1KO hearts. (e) Left ventricular (LV) systolic function quantified by ejection fraction (EF) and fractional shortening (FS). (f) Wheat germ agglutinin (WGA) staining and cell size quantification. (g) Confocal image with z-stacking showing co-localization of pH3, TnnT2, and Hoechst in a Meis1KO heart at P14. Immunostaining showing sarcomere disassembly and normal sarcomeric structure in Meis1KO hearts. Graph shows quantification of the number of pH3<sup>+</sup>+TnnT2<sup>+</sup> nuclei. (h) Expression of Aurora B in Meis1KO cardiomyocytes at P14 and quantification of the number of Aurora B+TnnT2+ cardiomyocytes

### 11.2.3 MI in Meis1 Overexpressing Heart Limits Neonatal Heart Regeneration

To determine whether forced Meis1 expression can inhibit neonatal cardiomyocyte proliferation, we generated a cardiac-specific Meis1 overexpressing mouse (Meis1 OE) by crossing pTRE-Meis1 mice with  $\alpha$ MHC-tTA mice to allow for specific overexpression of Meis1 in cardiomyocytes (Fig. 11.3a) around birth in the absence of tetracycline. We used a Meis1 line that overexpressed Meis1 by 2.5-fold (Fig. 11.3b). Overexpression of Meis1 did not result in a significant increase in heart-to-body weight ratio (Fig. 11.3c, d), normal systolic function (Fig. 11.3e), and increased cardiomyocyte size (Fig. 11.3f). Despite the increase in cardiomyocyte size in Meis1 (OE) hearts, the lack of decrease in heart-to-body weight ratio most probably reflects a decrease in the number of cardiomyocytes. This is supported by a decrease in the number of mitotic cardiomyocytes in the neonatal Meis1 (OE) hearts (Fig. 11.3g). More notably, Meis1 OE inhibited neonatal heart regeneration following induction of MI at P1 (Fig. 11.3h–j), whereas the wild-type hearts regenerated normally. Finally, Meis1 OE in cardiomyocytes resulted in upregulation of CDK inhibitors, most significantly p21 (Cdkn1a) (Fig. 11.3k). These results indicate that Meis1 overexpression in the neonatal heart results in premature cardiomyocyte cell cycle arrest.

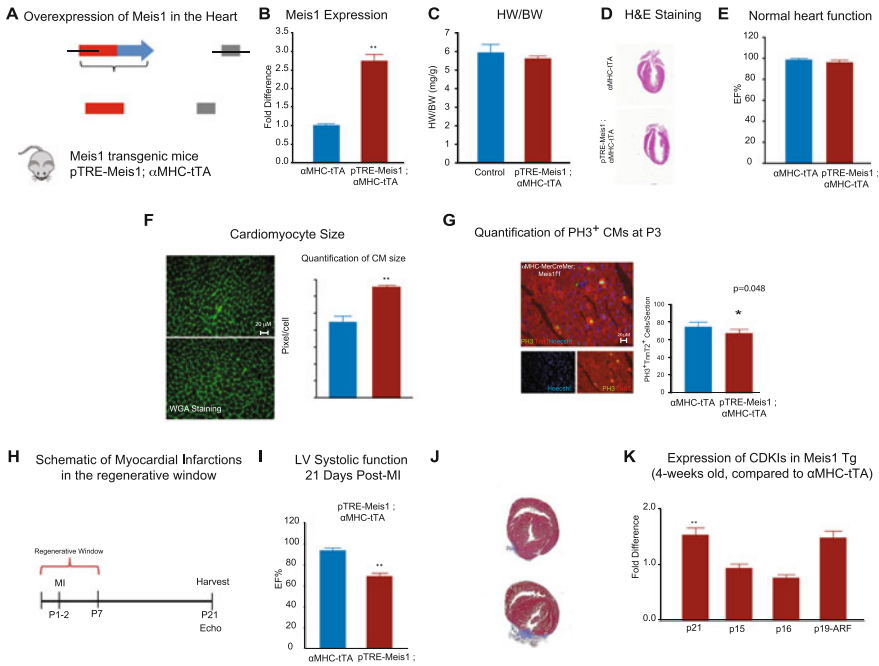


**Fig. 11.3** Meis1 overexpression limits neonatal heart regeneration following MI. (a) Schematic of Meis1 overexpression (OE) in the heart. Control mice were  $\alpha$ MHC-tTA, Meis1 (OE) mice were pTREMeis1- $\alpha$ MHC-tTA. (b) qRT-PCR demonstrates overexpression of Meis1. (c) HW-to-BW ratio in control and Meis1 (OE) mice. (d) H & E staining of WT and Meis1 (OE) hearts. (e) LV systolic function quantified by EF. (f) WGA staining and cell size quantification. (g) Immunostaining image showing co-localization of pH3, TnnT2, and Hoechst in Meis1 (OE) heart at P3. Graph shows quantification of pH3+TnnT2+ nuclei. (h) Schematic of neonatal MI during the regenerative window at P1. (i) LV systolic function of WT and Meis1 (OE) hearts at 21 days post-MI. (j) Trichromes at day 21 post-MI. (k) qRT-PCR of CDKIs in hearts of Meis1 (OE) compared to control

### 11.2.4 Regulation of Cyclin-Dependent Kinase Inhibitors by Meis1

In order to determine the mechanism by which Meis1 regulates cardiomyocyte proliferation, we performed a cell cycle PCR array. We found that Meis1 deletion resulted in downregulation of cyclin-dependent kinase inhibitors in isolated cardiomyocytes, including members of the Ink4b–Arf–Ink4a locus (p16, p15, and p19ARF) and CIP/ KIP family (p21 and p57), as well as upregulation of a number of positive regulators of the cell cycle (Fig. 11.3a, b). qRT-PCR confirmed these results (Fig. 11.4a). Of all the dysregulated cell cycle genes, we identified conserved Meis1 consensus binding sequences in the promoter region of only two loci, namely, the Ink4b–Arf–Ink4a (which includes p16INK4a, p19ARF, and p15INK4b) (Fig. 11.4b) and p21 loci (Fig. 11.4c) using the UCSC genome browser (<http://genome.ucsc.edu>). To test if Meis1 can transcriptionally activate Ink4b–

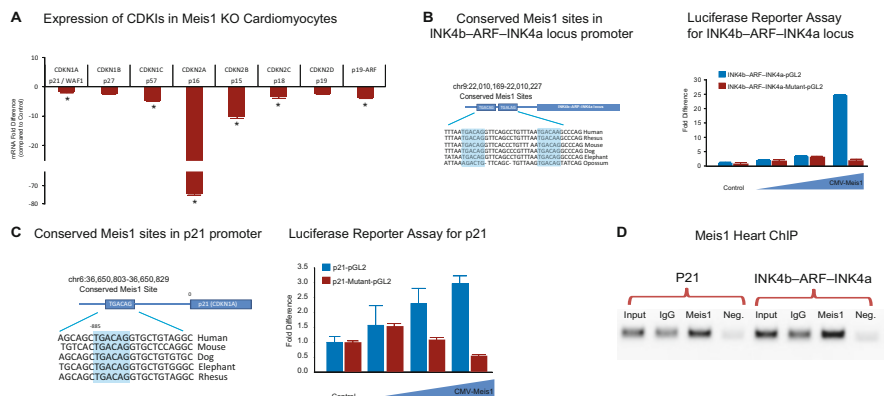


**Fig. 11.4** Regulation of cyclin-dependent kinase inhibitors by Meis1. (a) qPCR of CDKIs in purified Meis1 KO cardiomyocytes demonstrates significant downregulation of CDKN1A (p21), CDKN2B (p15), CDKN2A (p16), p19ARF, CDKN2C (p18), and CDKN1C (p57). (b) Highly conserved Meis1 motifs located in p16INK4a/p19ARF/p15INK4b promoter and luciferase reporter assay for INK4b-ARF-INK4a promoter demonstrating induction of INK4b-ARF-INK4a pGL2 reporter by Meis1 and loss of reporter activity following induction of mutation of Meis1 motifs (INK4b-ARF-INK4a-Mutant). (c) Highly conserved Meis1 motif located in p21 promoter and luciferase assay for p21 demonstrating induction of p21 pGL2 reporter by Meis1 and loss of reporter activity following mutation of Meis1 motifs (p21 Mutant). (d) *In vivo* confirmation of Meis1 interaction with INK4a/ARF/INK4b and p21 promoters by ChIP assay

Arf-INK4a and p21, we generated luciferase reporter constructs containing the conserved Meis1 binding motifs. Luciferase reporter assays with INK4b-ARF-INK4a-pGL2 (Fig. 11.4b) and p21-pGL2 reporters (Fig. 11.4c) demonstrated a dose-dependent activation by Meis1. Mutation of the putative Meis1 binding sites abolished the Meis1-dependent activation of the luciferase reporters (Fig. 11.4b, c). Finally, we demonstrated an *in vivo* interaction between Meis1 and Ink4b-Arf-INK4a and p21 promoters in the adult mouse heart by ChIP (Figs. 11.4d and 11.5).

### 11.3 Future Direction and Clinical Implications

The current study identifies Meis1 as a critical transcriptional regulator of cardiomyocyte cell cycle, upstream of two synergistic CDKI inhibitors. Although the mechanism of activation of Meis1 in the postnatal heart is not quite fully understood, results have demonstrated that Meis1 expression coincides with Hox genes that are known to interact with Meis1, stabilize its DNA binding, and enhance its transcriptional activity. Therefore, it would be important for future studies to define the transcriptional network involved in mediating the effect of Meis1 on postnatal cardiomyocytes. Ultimately, we hope to utilize our understanding of the role and mechanism of Meis1 in cardiomyocyte proliferation to uncover new disease mechanisms and therapeutic approaches for cardiovascular diseases.



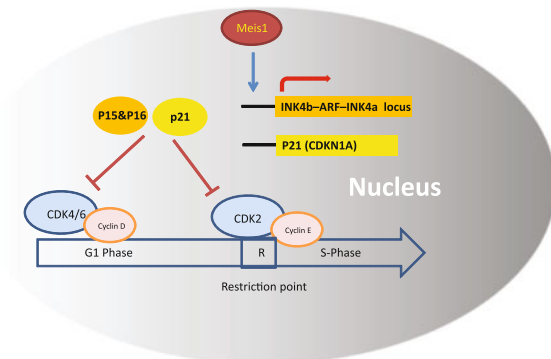


**Fig. 11.5** Proposed model of cardiomyocyte cell cycle regulation by Meis1. Meis1 regulates cardiomyocyte cell cycle arrest through transcriptional activation of CDKIs, INK4b-ARF-INK4a locus, and p21, as well as indirectly through a number of other cell cycle regulators. Activation of CDKIs leads to cell cycle arrest by inhibiting CDKs. Statistical significance: Values presented as mean  $\pm$  SEM. A Student's *t* test was used to determine statistical significance. \* $P < 0.05$ . \*\* $P < 0.01$

**Acknowledgments** We apologize to whose work was not cited in this chapter and for the omission of some discussion points owing to space constraints. This work was supported by grants from the AHA (Grant in Aid) (Sadek), the Gilead Research Scholars Program in Cardiovascular Disease (Sadek), Foundation for Heart Failure Research, NY, and the NIH (1R01HL115275-01) (Sadek).

**Open Access** This chapter is distributed under the terms of the Creative Commons Attribution-Noncommercial 2.5 License (<http://creativecommons.org/licenses/by-nc/2.5/>) which permits any noncommercial use, distribution, and reproduction in any medium, provided the original author(s) and source are credited.

The images or other third party material in this chapter are included in the work's Creative Commons license, unless indicated otherwise in the credit line; if such material is not included in the work's Creative Commons license and the respective action is not permitted by statutory regulation, users will need to obtain permission from the license holder to duplicate, adapt or reproduce the material.

## References

1. Porrello ER, et al. Transient regenerative potential of the neonatal mouse heart. *Science*. 2011;331(6020):1078–80.
2. Porrello ER, et al. Regulation of neonatal and adult mammalian heart regeneration by the miR-15 family. *Proc Natl Acad Sci U S A*. 2013;110(1):187–92.
3. Paige SL, et al. A temporal chromatin signature in human embryonic stem cells identifies regulators of cardiac development. *Cell*. 2012;151(1):221–32.
4. Wamstad JA, et al. Dynamic and coordinated epigenetic regulation of developmental transitions in the cardiac lineage. *Cell*. 2012;151(1):206–20.
5. Beltrami AP, et al. Evidence that human cardiac myocytes divide after MI. *N Engl J Med*. 2001;344(23):1750–7.

6. Bergmann O, et al. Evidence for cardiomyocyte renewal in humans. *Science*. 2009;324(5923):98–102.
7. Bergmann O, et al. Cardiomyocyte renewal in humans. *Circ Res*. 2012;110(1):p. e17–8; author reply e19–21.
8. Soonpaa MH, Field LJ. Assessment of cardiomyocyte DNA synthesis in normal and injured adult mouse hearts. *Am J Physiol*. 1997;272(1 Pt 2):H220–6.
9. Li F, et al. Rapid transition of cardiac myocytes from hyperplasia to hypertrophy during postnatal development. *J Mol Cell Cardiol*. 1996;28(8):1737–46.
10. Walsh S, et al. Cardiomyocyte cell cycle control and growth estimation in vivo – an analysis based on cardiomyocyte nuclei. *Cardiovasc Res*. 2010;86(3):365–73.
11. Moskow JJ, et al. Meis1, a PBX1-related homeobox gene involved in myeloid leukemia in BXH-2 mice. *Mol Cell Biol*. 1995;15(10):5434–43.
12. Argiropoulos B, Yung E, Humphries RK. Unraveling the crucial roles of Meis1 in leukemogenesis and normal hematopoiesis. *Genes Dev*. 2007;21(22):2845–9.
13. Imamura T, et al. Frequent co-expression of HoxA9 and Meis1 genes in infant acute lymphoblastic leukaemia with MLL rearrangement. *Br J Haematol*. 2002;119(1):119–21.
14. Pineault N, et al. Differential expression of Hox, Meis1, and Pbx1 genes in primitive cells throughout murine hematopoietic ontogeny. *Exp Hematol*. 2002;30(1):49–57.
15. Azcoitia V, et al. The homeodomain protein Meis1 is essential for definitive hematopoiesis and vascular patterning in the mouse embryo. *Dev Biol*. 2005;280(2):307–20.
16. Hisa T, et al. Hematopoietic, angiogenic and eye defects in Meis1 mutant animals. *EMBO J*. 2004;23(2):450–9.
17. Poolman RA, Gilchrist R, Brooks G. Cell cycle profiles and expressions of p21CIP1 AND P27KIP1 during myocyte development. *Int J Cardiol*. 1998;67(2):133–42.
18. Pasumarthi KB, et al. Targeted expression of cyclin D2 results in cardiomyocyte DNA synthesis and infarct regression in transgenic mice. *Circ Res*. 2005;96(1):110–8.
19. Gude N, et al. Akt promotes increased cardiomyocyte cycling and expansion of the cardiac progenitor cell population. *Circ Res*. 2006;99(4):381–8.
20. Sdek P, et al. Rb and p130 control cell cycle gene silencing to maintain the postmitotic phenotype in cardiac myocytes. *J Cell Biol*. 2011;194(3):407–23.

---

# Intercellular Signaling in Cardiac Development and Disease: The NOTCH pathway

# 12

Guillermo Luxán, Gaetano D'Amato, and José Luis de la Pompa

---

## Abstract

The heart is the first organ to develop in the embryo, and its formation is an exquisitely regulated process. Inherited mutations in genes required for cardiac development may cause congenital heart disease (CHD), manifested in the newborn or in the adult. Notch is an ancient, highly conserved signaling pathway that communicates adjacent cells to regulate cell fate specification, differentiation, and tissue patterning. Mutations in Notch signaling elements result in cardiac abnormalities in mice and humans, demonstrating an essential role for Notch in heart development. Recent work has shown that endocardial Notch activity orchestrates the early events as well as the patterning and morphogenesis of the ventricular chambers in the mouse and that inactivating mutations in the NOTCH pathway regulator MIND BOMB-1 (MIB1) cause left ventricular non-compaction (LVNC), a cardiomyopathy of poorly understood etiology. Here, we review these data that shed some light on the etiology of LVNC that at least in the case of that caused by *MIB1* mutations has a developmental basis.

---

## Keywords

Ventricles • Trabeculation • Compaction • Cardiomyopathy • LVNC • NOTCH

---

G. Luxán, PhD • G. D'Amato, MSc • J.L. de la Pompa, PhD (✉)

Intercellular Signalling in Cardiovascular Development & Disease Laboratory, Centro Nacional de Investigaciones Cardiovasculares (CNIC), Melchor Fernández Almagro 3, 28029 Madrid, Spain

e-mail: [jlpompa@cnic.es](mailto:jlpompa@cnic.es)

© The Author(s) 2016

T. Nakanishi et al. (eds.), *Etiology and Morphogenesis of Congenital Heart Disease*, DOI 10.1007/978-4-431-54628-3\_12

103

## 12.1 Introduction

Heart development begins in the mouse at embryonic day 7 (E7) when pre-cardiac precursor cells move forward bilaterally into the lateral plate mesoderm to form the cardiac crescent [14]. By E8, a linear heart tube is formed after folding of the mesodermal layers from both sides of the embryo, and the two main tissues of the heart are present, the endocardium inside and the outer myocardium. At E9.0, the heart loops and grows by addition of cells from both cardiac poles [20]. At E9.5, the heart divides afterward into developmental domains that would allow the formation of two regions, the valve and the chamber regions [24] (Fig. 12.1a).

We will describe in some detail the process of ventricular chamber development because it is the focus of this review. At E9.5, the process of trabeculation begins in the primitive ventricles. Trabeculae are highly organized sheets of cardiomyocytes that protrude toward the light of the ventricles [3]. Trabeculae are the first structural landmark of the developing ventricles [31]. They increase the ventricular surface and allow the myocardium to grow in the absence of coronary vessels that will be formed later. Trabeculae are important for contractibility, formation of the conduction system, and blood flow direction in the ventricle. Although trabeculae start to form first in the left ventricle and later in the right ventricle, there are no differences between these structures in the two ventricles. Formed trabeculae have no free ends and they make the ventricle appear like a sponge [31] (Fig. 12.1b). From E10.5 onward, the ventricular myocardium has two well-defined regions, morphologically and molecularly, the outer compact myocardium and the inner trabecular layer. The compact myocardium is less differentiated and shows a higher proliferation rate than the trabecular myocardium [31]. Differentiated cardiomyocytes will give rise to the working myocardium and the conduction system [31]. After completion of ventricular septation around E14.5, further growth and maturation of the ventricular chambers require a complete trabecular remodeling and reorganization into an apico-basal orientation that determines the shape of the ventricles (Fig. 12.1c). Trabeculae become compacted and as a result there is a significant change in the ratio of compact vs. trabecular myocardium in the ventricle. Trabeculae compaction is accompanied by the hypoxia-dependent invasion of the coronary vasculature from the epicardium into the compact layer of the myocardium [33]. As they compact, the intertrabecular recesses are transformed into capillaries of the rising coronary plexus. This is followed by a reorganization of the muscle fibers of the heart that organize in a three-layered spiral around the heart reflecting the twisting pattern of heart contraction [31]. Trabeculae stop proliferating while the proliferation of the compact zone sustains the growth of the chamber and the contribution of the compact layer to the heart becomes more significant than the one of the luminal trabeculations that will eventually disappear. How exactly this happens and what molecular mechanisms drive this process is unknown.

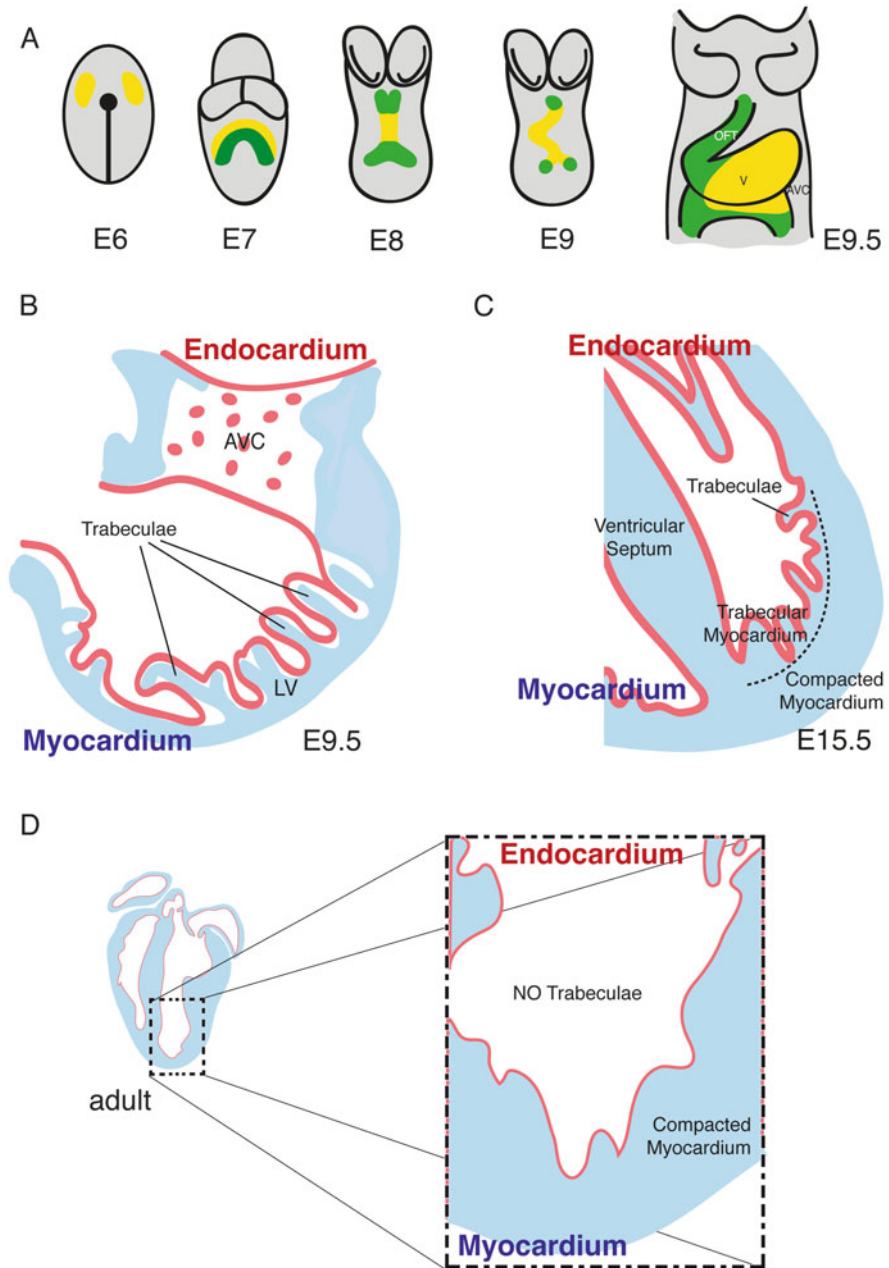


**Fig. 12.1** Overview of early heart development. (a) Ventral views of the developing mouse embryo. At E7.0, cardiac progenitors (*yellow*) migrate to the center of the embryo to form the cardiac tube and at E7.5, two cardiac fields can be distinguished: the first heart field (FHF; *yellow*) and the second heart field (SHF; *green*). By E8.0, the cardiac tube is formed where endocardium and myocardium are already present. At E9.0 the tube loops and at E9.5, has four anatomically distinct regions: atrium, atrioventricular canal (AVC), ventricle (V), and outflow tract (OFT).

## 12.2 Left Ventricular Non-compaction (LVNC)

LVNC is a cardiomyopathy of poorly understood etiology that is characterized by prominent and excessive trabeculations with deep recesses in the ventricular wall [18]. LVNC was first diagnosed in 1984, in a 33-year-old woman assessed by echocardiography [10]. Since then, the heterogeneity of its symptoms might have left many LVNC cases undiagnosed [18], giving a lower estimation of its real impact as a cardiomyopathy. The improvement in imaging technologies and the advent of CMRI allow now a better diagnosis of this disease, and 10 years after the first description, LVNC was included in the World Health Organization (WHO) catalogue of cardiomyopathies [30]. In 2006, the American Heart Association included LVNC to its list of genetic cardiomyopathies caused by an arrest of the normal compaction process of the developing myocardium [23]. LVNC can be almost asymptomatic or manifest as depressed systolic function [7], accompanied by systemic embolism, malignant arrhythmias, heart failure, and sudden death [25], although its clinical manifestation and the age of the affected individual at symptom onset are variable. LVNC was shown to be caused by mutations in genes encoding mainly structural proteins of the cardiac muscle, cytoskeleton, nuclear membrane, and chaperone proteins. In general, familial forms of LVNC are transmitted as an autosomal-dominant trait [7]. The underlying molecular mechanisms that produce the structural abnormalities leading to LVNC are still unknown [34].

---

## 12.3 The NOTCH Signaling Pathway

Notch is a conserved signaling pathway that regulates cell fate specification, differentiation, and tissue patterning via local cell interactions [2]. There are four Notch receptors in mammals, Notch1–Notch4, which are expressed in different tissues and at different times during embryonic and adult life. Notch is a large type I transmembrane receptor that has two distinct domains, an extracellular domain (NECD) responsible for the interaction with the ligands and an intracellular domain (NICD) responsible for signal transduction (Fig. 12.2). NECD contains a varied number of tandem arrays of epidermal growth factor (EGF)-like repeats [2]. NICD is composed of the RAM23 domain and 6 ankyrin repetitions responsible for the interaction with RBPJK, the transcriptional effector of the pathway; two nuclear localization signals; a transcriptional activation domain only present in Notch1 and Notch2; and a terminal PEST domain that negatively regulates the stability of the receptor [21]. NECD and NICD are synthesized as a single polypeptide, which is directly cleaved after translation by a furin convertase in the Golgi. This first

---

**Fig. 12.1** (continued) Endocardial cushions are formed in valvulogenic regions of the heart (*green*, OFT and *blue*, AVC) and trabeculae appear in the ventricles (**b**). At E15.5, trabeculae are undergoing compaction and there is a thick compact myocardium (**c**) that becomes very prominent in the adult ventricle that has a smooth surface (**d**)

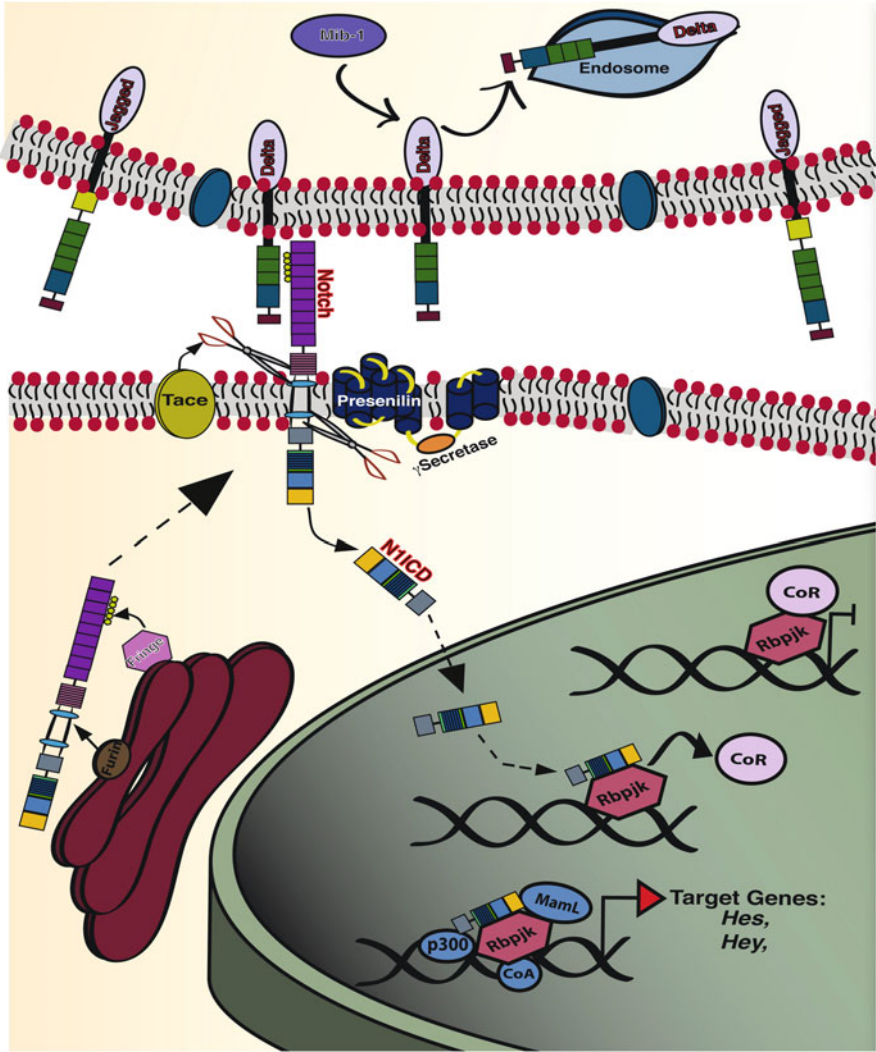


**Fig. 12.2** The Notch signaling pathway. The Notch ligands Delta and Jagged are tethered to the membrane of the signaling cell. On their way to the plasmatic membrane, the Notch receptors are modified in their extracellular domains (NECD) by Fringe. Upon ligand-receptor interaction, Mib1 ubiquitylates the ligand, targeting it for endocytosis. Pulling of NECD allows the cleavage and release of NICD by  $\gamma$ -secretase. NICD translocates to the nucleus and forms a transcriptional activation complex together with RBPJK and MAML that activates target genes transcription, including *Hes* and *Hey* that encode transcriptional repressors

cleavage [6] is necessary to form the functional heterodimeric receptor that will be translocated to the membrane where the two domains are still associated by  $\text{Ca}^{2+}$ -dependent non-covalent bonds [28]. In mammals, the Notch ligands belong to the Delta-like (Dll1, Dll3, and Dll4) and Jagged (Jag1 and Jag2) families. The ligands

are type I transmembrane proteins and their extracellular domains are composed by a repetition of EGF-like domains responsible for the interaction with the receptor and the DSL (Delta, Serrate, Lin12) domain (Fig. 12.2) [21]. The glycosyltransferase Fringe can modify the EGF-like domain in the NECD of the receptor by adding O-fucose glycans [5] (Fig. 12.2). This modification determines which ligand preferentially binds to the receptor. There is evidence that the presence of Fringe shifts the activation balance toward Delta-like ligands at the expense of Jagged ligands when both molecules are expressed at the same time in the same tissue [4]. The E3 ubiquitin ligase Mind bomb1 (Mib1) regulates the endocytosis of the Notch ligands when bound to NECD, a prerequisite for Notch activation [16]. Mib1 binds to the two families of Notch ligands, and it is a point of regulation of the pathway in the signaling cell. Upon interaction of ligand and receptor, Mib1 targets by ubiquitylation the ligand for endocytosis [16]. The ligands are endocytosed, mechanically pulling NECD producing a conformational change that exposes a second cleavage site [27] allowing a metalloprotease of the ADAM family to cleave NECD [13] that is finally endocytosed into the signaling cell together with the ligand. Immediately after,  $\gamma$ -secretase/Presenilin cleaves the receptor in a third site liberating the NICD in the cytoplasm of the receiving cell [26] (Fig. 12.2). NICD translocates to the nucleus where it binds to the transcription factor CSL or RBPJK via by the RAM23 domain [32]. In the absence of Notch signaling activation, RBPJK is bound to nuclear corepressors that inhibit gene expression. Upon the interaction of NICD with RBPJK, the transcriptional repressors are released and transcriptional activators such as Master mind-like (Maml) [35] are recruited forming a protein complex that activates the expression of target genes (Fig. 12.2).

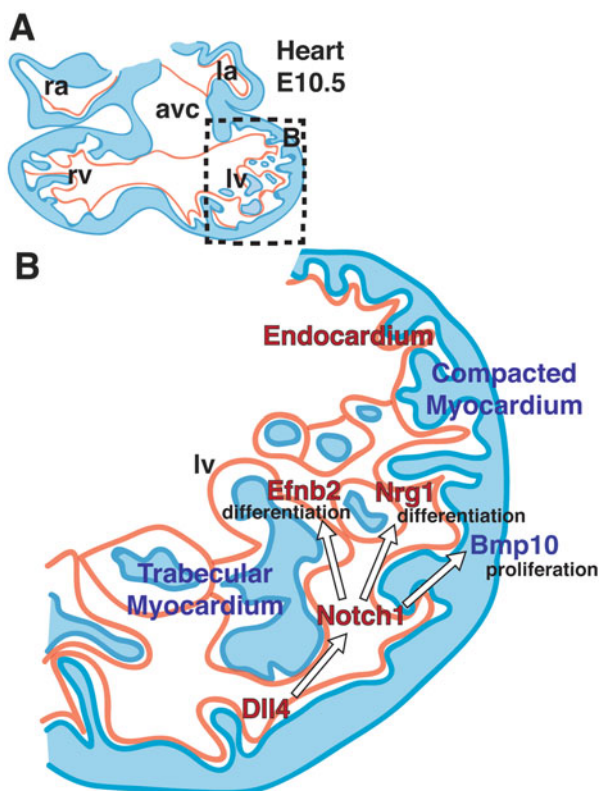
---

## 12.4 NOTCH in Ventricular Chamber Development

Notch pathway elements show a complex expression pattern in the developing mouse chambers. At E9.5, Mib1 is expressed in endocardium and myocardium, Dll4 in the endocardium especially at the base of the forming trabeculae, Jag1 in the myocardium, and N1ICD is only active at discrete sites where the trabeculae form [9]. Analysis of standard and endothelial-specific *Notch1* and *RBPJK* mutants shows that trabeculation is severely impaired and only primitive, poorly organized trabeculae can be observed in these mutants [12]. Molecular analysis indicates that during trabeculation, Notch modulates three different signals: EphrinB2 [1], expressed in the endocardium, is a direct Notch target. Nrg1 [15], also expressed in the endocardium, is an indirect Notch target, and its expression depends both of Notch and EphrinB2 [12]. Nrg1 induces the formation of the ventricular conduction system, a feature of ventricular maturation [29]. A third signaling pathway is Bmp10 [8], expressed in trabecular myocardium and whose expression is severely downregulated in Notch pathway mutants, suggesting that Notch is required to produce a signal that activates Bmp10 in the myocardium [12]. During these early



**Fig. 12.3** Proposed mechanism of Notch function in trabeculation. (a, b detail) Dll4 activates Notch1 at the base of the developing trabeculae. N1ICD/RBPJK activates EphrinB2(Efnb2)/EphB4 signaling in the endocardium, which in turn is required for Nrg1 expression in this tissue. Nrg1 activates ErbB2/ErbB4 signaling in myocardium to promote cardiomyocyte differentiation. In addition, Notch1 signaling in endocardium is required for Bmp10 expression and therefore proliferation of trabecular cardiomyocytes (Modified from [12])



stages, the ligand Dll4 is the main Notch activator in the endocardium [12] (Fig. 12.3).

To precisely determine the contribution of Notch ligands to ventricular chamber development, we bred mice bearing a conditional allele of *Mib1* with myocardium-specific Cre driver line *cTnT-Cre* [19]. Histological examination at E16.5 revealed that *Mib1<sup>fllox</sup>;cTnT-Cre* mutants had a dilated heart with a thin compact myocardium and large, non-compacted trabeculae, protruding toward the ventricular lumen. Morphological and functional analysis using echocardiography and cardiac magnetic resonance imaging (CMRI) showed prominent trabeculations, deep intertrabecular recesses, and a significantly reduced ejection fraction in mutant mice [22]. The hearts of these mice had a ratio of non-compacted to compacted myocardium (non-compaction index, NC) of 2.0, a feature diagnostic of LVNC in humans [11, 17]. These features are all strongly reminiscent of LVNC, establishing *Mib1<sup>fllox</sup>;cTnT-Cre* mice as the first animal model of LVNC [22]. Analysis of chamber markers in E15.5 *Mib1<sup>fllox</sup>;cTnT-Cre* mice revealed expansion of various compact myocardium markers (*Hey2*, *Tbx20* and *n-myc*) to the trabeculae and

reduced expression of the trabecular markers *Anf*, *Bmp10*, and *Cx40*. These markers were normally expressed at earlier stages, suggesting that maintenance of trabecular maturation and patterning is impaired in *Mib1<sup>fllox</sup>;cTnT-Cre* mutants. Likewise, lost or reduced *Hey1*, *Hey3*, and *EphrinB2* expression in the vessels of the compact myocardium suggested that coronary artery development was defective. Proliferation analysis revealed increased proliferation of trabecular cardiomyocytes in the hearts of E15.5 *Mib1<sup>fllox</sup>;cTnT-Cre* embryos, suggesting this as the cause of the enlarged, non-compacted trabeculae in these mutants. RNA sequencing analysis of E14.5 *Mib1<sup>fllox</sup>;cTnT-Cre* mutant ventricles identified altered expression of 315 genes (132 upregulated and 183 downregulated). The expression of genes involved in the differentiation of cardiac endothelium/endothelium and cardiomyocytes and coronary vasculogenesis was altered. RNA-Seq data also confirmed the in situ hybridization analysis and demonstrated that *Mib1* inactivation in the myocardium disrupts the differentiation and maturation of cardiac endothelial cells and cardiomyocytes. This may impact in turn the process of ventricular maturation and compaction. Genetic ablation of *Mib1* in the myocardium thus leads to LVNC cardiomyopathy in mice by arresting ventricular trabeculae maturation and compaction and increasing cardiomyocyte proliferation during fetal development [22].

We next examined whether mutations in the human *MIB1* homologue were associated with clinical LVNC and identified two mutations in a cohort of 100 Southern European LVNC cases; one was a heterozygous G to T transversion of nucleotide 2827 in exon 20 (causing a change in amino acid 943 from valine to phenylalanine, the p.Val943Phe mutation). Val943 is located within a region that mediates protein-protein interactions and constitutes the site of MIB1 ubiquitin ligase activity. The second mutation was a heterozygous C to T transition of nucleotide 1587 in *MIB1* exon 11 (causing a premature stop codon instead of arginine at position 530 in the MIB1 ankyrin repeats region, the p.Arg530X mutation). These two mutations were tracked back through three and two generations of LVNC-affected individuals, revealing co-segregation with LVNC, confirming the hereditary nature of the disease [22].

In silico modeling suggested that MIB1 is a homodimer where the p.Val943Phe mutant will alter the alignment of the ring finger domains in heterodimers formed by wild-type and mutant p.Val943Phe MIB1, as well as the angle of interaction with JAG1 of the p.Val943Phe wild-type dimers. This possibility was supported by co-immunoprecipitation experiments with tagged wild-type MIB1 and mutant MIB1 isoforms co-transfected in pair-wise combinations into HEK293 cells. The effect of the *MIB1* mutations on Jag1 ubiquitylation was tested also in HEK293 cells. Jag1 ubiquitylation was strongly reduced in cells co-transfected with wild-type MIB1 plus p.Val943Phe or wild-type MIB1 plus the p.Arg530X mutant [22].

Lastly, to study the effect of these mutant *MIB1* variants in vivo, their mRNAs were microinjected into zebra fish embryos expressing GFP in the developing myocardium. Examination of 72 hpf larvae injected with p.Val943Phe or p.Arg530X mRNAs revealed severely disrupted embryonic development, disrupted cardiac looping, and kinked tail, typical of defective Notch activity. To complement

these findings, we cocultured Jag1-HEK293 cells expressing MIB1 variants with *Notch1*-expressing HEK293 cells co-transfected with a Notch luciferase reporter. Jag1-HEK293 cells expressing wild-type *MIB1* increased Notch reporter activity, whereas the p.Val934Phe and p.Arg530X mutant forms reduced reporter activity, indicating that both human mutations disrupt Notch signaling [22].

Accumulated data suggested that both *MIB1* mutations result in loss of MIB1 WT function. In the case of p.Arg530X, this would be due to haploinsufficiency caused by insufficient synthesis of WT MIB1 protein; in the case of p.Val934Phe, this would be due to a dominant-negative effect of the mutant protein, titrating down the amount of functional WT MIB1 dimers through heterotypic or homotypic interactions. In both cases, loss of MIB1 function leads to disease inherited in an autosomal-dominant fashion.

As to the role of *Mib1* in ventricular chamber development, we have proposed that myocardial *Mib1* activity enables Jag1-mediated activation of *Notch1* in the endocardium, to sustain trabeculae patterning, maturation, and compaction [22] and (Fig. 12.4). Abrogation of *Mib1*-mediated signaling in the myocardium disrupts trabeculae maturation and patterning, arresting the development of chamber myocardium and resulting in LVNC (Fig. 12.4). The expansion of compact zone markers to the trabeculae of E15.5 *Mib1<sup>fllox</sup>;cTnT-Cre* mutants further suggests that trabeculae patterning and maturation is impaired (Fig. 12.4). In addition, the disruption of coronary vessel markers in *Mib1<sup>fllox</sup>;cTnT-Cre* mutants indicates that abrogation of myocardial-endocardial Notch signaling indirectly impairs coronary vessel formation.

---

## 12.5 Future Directions and Clinical Implications

The data reviewed here establish the causal role of NOTCH dysregulation in LVNC, a congenital cardiomyopathy that results from a developmental arrest in ventricular maturation and myocardial compaction. These findings will lead to a better diagnosis and risk stratification, allowing timely intervention in LVNC-associated complications. In addition, since other NOTCH pathway elements may be involved in LVNC, they could serve as novel diagnostic or therapeutic disease targets. Further research is required to determine the molecular mechanisms and regulatory interactions underlying NOTCH function in ventricular chamber development using genetically modified mouse models and the full implication of altered NOTCH signaling in human LVNC.

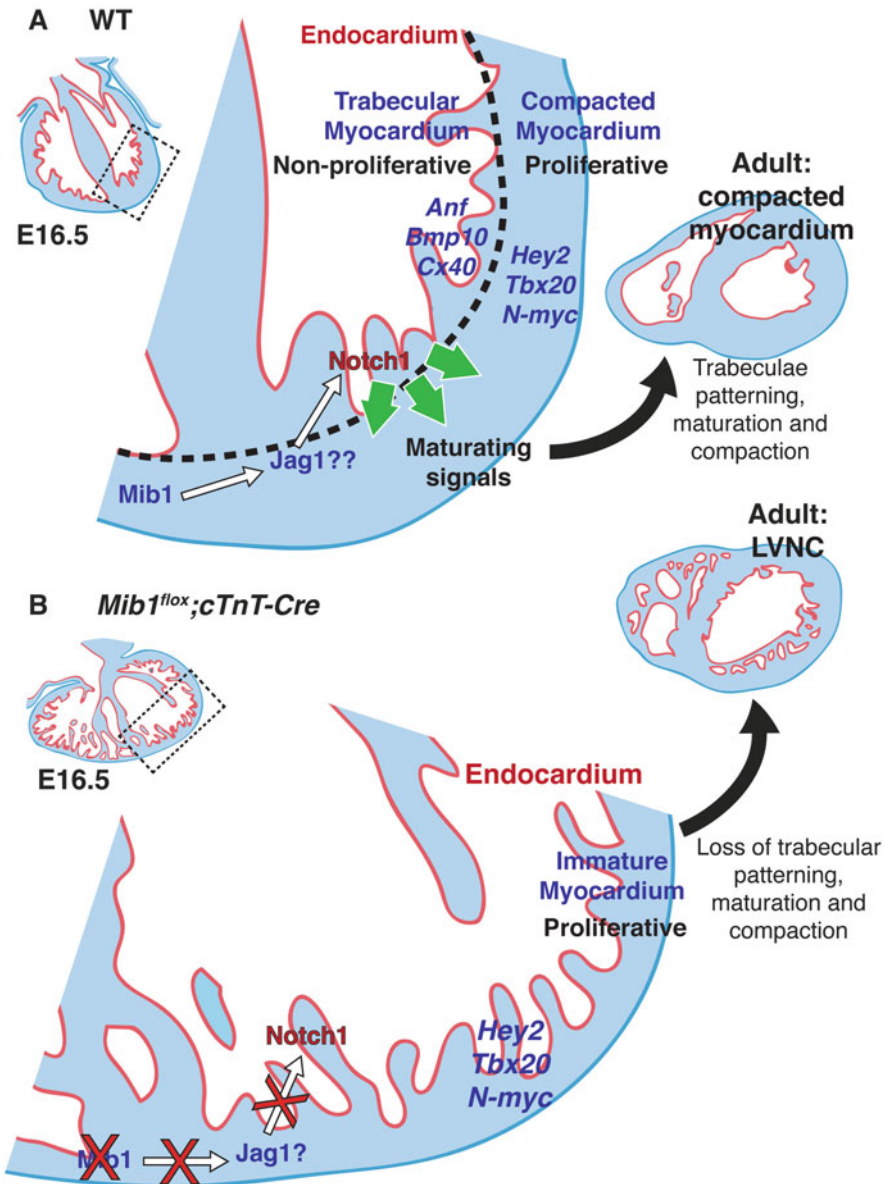


**Fig. 12.4** Proposed mechanism of Notch function in trabecular maturation and compaction. (a) In wild-type (WT) embryos, ubiquitylation of Jag1 (and another ligand?) by Mib1 in the myocardium allows Notch1 activation in the endocardium. N1ICD is required to sustain trabecular patterning, maturation, and compaction. The compact myocardium (expressing *Hey2*, *Tbx20* and *n-myc*) proliferates actively, unlike the trabecular myocardium (expressing *Anf*, *Bmp10* and *Cx40*). Notch-dependent chamber maturation leads to compacted ventricular myocardium in the adult mouse. (b) In *Mib1<sup>flox</sup>; cTnT-Cre* mutants, Notch1 activity is impaired and compact myocardium markers (*Hey2*, *Tbx20* and *n-myc*) are consequently expanded to the trabeculae, which remain abnormally proliferative. The resulting disruption of trabecular patterning, maturation, and compaction manifests as LVNC (Modified from [22])

**Acknowledgments** We apologize to those authors whose work was not cited. J.L. de la Pompa is funded by grants SAF2013-45543, RD12/0042/0005 (RIC), and RD12/0019/0003 (TERCEL) from the Spanish Ministry of Economy and Competitiveness (MINECO) and grant FP7-ITN 215761 (NotchIT) from the European Commission. G. Luxán had a PhD fellowship from the MINECO (FPI Program, ref. BES-2008-002904) and G. D’Amato holds a PhD fellowship associated with grant FP7-ITN 215761 (NotchIT). The CNIC is supported by the MINECO and the Pro-CNIC Foundation.

**Open Access** This chapter is distributed under the terms of the Creative Commons Attribution-Noncommercial 2.5 License (<http://creativecommons.org/licenses/by-nc/2.5/>) which permits any noncommercial use, distribution, and reproduction in any medium, provided the original author(s) and source are credited.

The images or other third party material in this chapter are included in the work’s Creative Commons license, unless indicated otherwise in the credit line; if such material is not included in the work’s Creative Commons license and the respective action is not permitted by statutory regulation, users will need to obtain permission from the license holder to duplicate, adapt or reproduce the material.

---

## References

1. Adams RH, Wilkinson GA, Weiss C, et al. Roles of ephrinB ligands and EphB receptors in cardiovascular development: demarcation of arterial/venous domains, vascular morphogenesis, and sprouting angiogenesis. *Genes Dev.* 1999;13:295–306.
2. Artavanis-Tsakonas S, Rand MD, Lake RJ. Notch signaling: cell fate control and signal integration in development. *Science.* 1999;284:770–6.
3. Ben-Shachar G, Arcilla RA, Lucas RV, et al. Ventricular trabeculations in the chick embryo heart and their contribution to ventricular and muscular septal development. *Circ Res.* 1985;57:759–66.
4. Benedito R, Roca C, Sorensen I, et al. The notch ligands Dll4 and Jagged1 have opposing effects on angiogenesis. *Cell.* 2009;137:1124–35.
5. Blair SS. Notch signaling: fringe really is a glycosyltransferase. *Curr Biol.* 2000;10:R608–12.
6. Blaumueller CM, Qi H, Zagouras P, et al. Intracellular cleavage of Notch leads to a heterodimeric receptor on the plasma membrane. *Cell.* 1997;90:281–91.
7. Captur G, Nihoyannopoulos P. Left ventricular non-compaction: genetic heterogeneity, diagnosis and clinical course. *Int J Cardiol.* 2010;140:145–53.
8. Chen H, Shi S, Acosta L, et al. BMP10 is essential for maintaining cardiac growth during murine cardiogenesis. *Development.* 2004;131:2219–31.
9. Del Monte G, Grego-Bessa J, Gonzalez-Rajal A, et al. Monitoring Notch1 activity in development: evidence for a feedback regulatory loop. *Dev Dyn.* 2007;236:2594–614.
10. Engberding R, Bender F. Identification of a rare congenital anomaly of the myocardium by two-dimensional echocardiography: persistence of isolated myocardial sinusoids. *Am J Cardiol.* 1984;53:1733–4.
11. Finsterer J, Stollberger C. Heterogenous myopathic background of left ventricular hypertrabeculation/noncompaction. *Am J Med Genet A.* 2004;131:221; author reply 222–223.
12. Grego-Bessa J, Luna-Zurita L, Del Monte G, et al. Notch signaling is essential for ventricular chamber development. *Dev Cell.* 2007;12:415–29.
13. Hartmann D, De Strooper B, Serneels L, et al. The disintegrin/metalloprotease ADAM 10 is essential for Notch signalling but not for alpha-secretase activity in fibroblasts. *Hum Mol Genet.* 2002;11:2615–24.
14. Harvey RP. Patterning the vertebrate heart. *Nat Rev Genet.* 2002;3:544–56.

15. Hertig CM, Kubalak SW, Wang Y, et al. Synergistic roles of neuregulin-1 and insulin-like growth factor-I in activation of the phosphatidylinositol 3-kinase pathway and cardiac chamber morphogenesis. *J Biol Chem.* 1999;274:37362–9.
16. Itoh M, Kim CH, Palardy G, et al. Mind bomb is a ubiquitin ligase that is essential for efficient activation of Notch signaling by Delta. *Dev Cell.* 2003;4:67–82.
17. Jenni R, Oechslin E, Schneider J, et al. Echocardiographic and pathoanatomical characteristics of isolated left ventricular non-compaction: a step towards classification as a distinct cardiomyopathy. *Heart.* 2001;86:666–71.
18. Jenni R, Oechslin EN, Van Der Loo B. Isolated ventricular non-compaction of the myocardium in adults. *Heart.* 2007;93:11–5.
19. Jiao K, Kulesa H, Tompkins K, et al. An essential role of Bmp4 in the atrioventricular septation of the mouse heart. *Genes Dev.* 2003;17:2362–7.
20. Kelly RG, Buckingham ME. The anterior heart-forming field: voyage to the arterial pole of the heart. *Trends Genet.* 2002;18:210–6.
21. Kopan R. Notch: a membrane-bound transcription factor. *J Cell Sci.* 2002;115:1095–7.
22. Luxan G, Casanova JC, Martinez-Poveda B, et al. Mutations in the NOTCH pathway regulator MIB1 cause left ventricular noncompaction cardiomyopathy. *Nat Med.* 2013;19:193–201.
23. Maron BJ, Towbin JA, Thiene G, et al. Contemporary definitions and classification of the cardiomyopathies: an American Heart Association Scientific Statement from the Council on Clinical Cardiology, Heart Failure and Transplantation Committee; Quality of Care and Outcomes Research and Functional Genomics and Translational Biology Interdisciplinary Working Groups; and Council on Epidemiology and Prevention. *Circulation.* 2006;113:1807–16.
24. Moorman AF, Christoffels VM. Cardiac chamber formation: development, genes, and evolution. *Physiol Rev.* 2003;83:1223–67.
25. Oechslin EN, Attenhofer Jost CH, Rojas JR, et al. Long-term follow-up of 34 adults with isolated left ventricular noncompaction: a distinct cardiomyopathy with poor prognosis. *J Am Coll Cardiol.* 2000;36:493–500.
26. Okochi M, Steiner H, Fukumori A, et al. Presenilins mediate a dual intramembranous gamma-secretase cleavage of Notch-1. *EMBO J.* 2002;21:5408–16.
27. Parks AL, Klueg KM, Stout JR, et al. Ligand endocytosis drives receptor dissociation and activation in the Notch pathway. *Development.* 2000;127:1373–85.
28. Rand MD, Grimm LM, Artavanis-Tsakonas S, et al. Calcium depletion dissociates and activates heterodimeric notch receptors. *Mol Cell Biol.* 2000;20:1825–35.
29. Rentschler S, Zander J, Meyers K, et al. Neuregulin-1 promotes formation of the murine cardiac conduction system. *Proc Natl Acad Sci U S A.* 2002;99:10464–9.
30. Richardson P, McKenna W, Bristow M, et al. Report of the 1995 World Health Organization/International Society and Federation of Cardiology Task Force on the Definition and Classification of cardiomyopathies. *Circulation.* 1996;93:841–2.
31. Sedmera D, Pexieder T, Vuillemin M, et al. Developmental patterning of the myocardium. *Anat Rec.* 2000;258:319–37.
32. Tamura K, Taniguchi Y, Minoguchi S, et al. Physical interaction between a novel domain of the receptor Notch and the transcription factor RBP-J kappa/Su(H). *Curr Biol.* 1995;5:1416–23.
33. Tao J, Doughman Y, Yang K, et al. Epicardial HIF signaling regulates vascular precursor cell invasion into the myocardium. *Dev Biol.* 2013;376:136–49.
34. Towbin JA. Left ventricular noncompaction: a new form of heart failure. *Heart Fail Clin.* 2010;6:453–69. viii.
35. Wu L, Aster JC, Blacklow SC, et al. MAML1, a human homologue of Drosophila mastermind, is a transcriptional co-activator for NOTCH receptors. *Nat Genet.* 2000;26:484–9.

---

# The Epicardium in Ventricular Septation During Evolution and Development

# 13

Robert E. Poelmann, Bjarke Jensen, Margot M. Bartelings,  
Michael K. Richardson, and Adriana C. Gittenberger-de Groot

---

## Abstract

The epicardium has several essential functions in development of cardiac architecture and differentiation of the myocardium in vertebrates. We uncovered a novel function of the epicardium in species with partial or complete ventricular septation including reptiles, birds and mammals. Most reptiles have a complex ventricle with three cava, partially separated by the horizontal and vertical septa. Crocodylians, birds and mammals, however, have completely separated left and right ventricles, a clear example of convergent evolution. We have investigated the mechanisms underlying epicardial involvement in septum formation in

---

R.E. Poelmann (✉)

Department of Anatomy and Embryology, Leiden University Medical Center, PO Box 9600, 2300RC Leiden, The Netherlands

Department of Cardiology, Leiden University Medical Center, PO Box 9600, 2300RC Leiden, The Netherlands

Institute of Biology Leiden (IBL), Leiden University, Sylvius Laboratory, Sylviusweg 72, 2333BE Leiden, The Netherlands

e-mail: [R.E.Poelmann@lumc.nl](mailto:R.E.Poelmann@lumc.nl)

B. Jensen

Department Anatomy, Embryology and Physiology, AMC, Amsterdam, The Netherlands

Department of Bioscience-Zoophysiology, Aarhus University, Aarhus, Denmark

M.M. Bartelings

Department of Anatomy and Embryology, Leiden University Medical Center, PO Box 9600, 2300RC Leiden, The Netherlands

M.K. Richardson

Institute of Biology Leiden (IBL), Leiden University, Sylvius Laboratory, Sylviusweg 72, 2333BE Leiden, The Netherlands

A.C.G.-d. Groot

Department of Cardiology, Leiden University Medical Center, PO Box 9600, 2300RC Leiden, The Netherlands

embryos. We find that the primitive ventricle of early embryos becomes septated by folding and fusion of the anterior ventricular wall, trapping epicardium in its core. This ‘folding septum’, as we propose to call it, develops in lizards, snakes and turtles into the horizontal septum and, in the other taxa studied, into the folding part of the interventricular septum. The vertical septum, indistinct in most reptiles, arises in crocodylians and pythonids at the posterior ventricular wall. It is homologous to the inlet septum in mammals and birds. Eventually, the various septal components merge to form the completely septated heart. In our attempt to discover homologies between the various septum components, we draw perspectives to the development of ventricular septal defects in humans.

---

**Keywords**

Evolution and development • Homology • Ventricular septum • Congenital heart disease • Epicardium

---

### 13.1 Introduction

Evolution of full division of the heart into left and right chambers by septa started with the atrium in amphibians, followed by the ventricle in amniotes. Full ventricular septation evolved independently in the lineages of the archosaurs, whose extant representatives are the birds and crocodylians and mammals [1]. Not only is evolution and development of ventricular septation of considerable biological interest, it is also of clinical relevance to the understanding of many types of ventricular septal defects in humans [2].

We demonstrated that part of the ventricular septum depends on interactions between myocardium and the epicardium including the epicardium-derived cells (EPDCs) for its development [3]. The septum will develop abnormally if the epicardium is disturbed [4, 5]. Ventricular development, starting with a primitive common ventricular tube, leading to separation into the left and right ventricle, involves complex mechanisms including the ventricular inflow and outflow compartment [6, 7]. Most reptile groups show a more primitive pattern comprising a horizontal and a vertical septum separating the ventricle into three interconnected cavities. How the primitive reptilian pattern was modified into the complete septum is a matter of debate. Here we report the functional role of the epicardium in ventricular septation in lizard, snake, turtle, chicken, mouse and human using descriptive and experimental approaches including quail-chicken chimeras by transplantation of quail proepicardial organ into the pericardial cavity of chicken [4]. Furthermore, epicardium-deficient animal models such as the podoplanin knockout mouse and epicardial ablation experiments in chicken embryos were investigated [4, 5]. With DiI labelling [8] of the myocardial surface in chicken embryos, the outgrowth of the cardiac compartments was analysed. *Tbx5* expression showed gradients along the cardiac tube and so may be a useful marker for regionalisation of the heart [9]. For experimental details and full material and method description, we refer to [10].



## 13.2 Septum Components in the Completely Septated Heart

Varying terminology is used for components of the ventricular septum and their respective boundaries; we adopted the following. The posterior component of the interventricular septum, between the left and right atrioventricular junctions, is the *inlet septum*. We propose to use the term ‘folding septum’ (newly defined here) for the anterior component. The septal band is a muscular ridge on the right ventricular septal surface between the inlet and folding septum, extending as the moderator band towards the right ventricular free wall. In the completely septated heart, the aortopulmonary septum is the last component that closes the interventricular communication, but has not been specifically studied here.

## 13.3 The Presence of the Epicardium in Amniotes

Among other species we examined embryos of Macklot’s python (*Liasis mackloti*), European pond turtle (*Emys orbicularis*) and Chinese soft-shell turtle (*Pelodiscus sinensis*). The presence of epicardium on the outer face of the myocardial heart tube is confirmed. A pronounced subepicardium in the inner curvature of the looping heart tube at the site of the bulboventricular fold is confirmed, here referred to as epicardial cushion, being almost as elaborate as the adjacent endocardial atrioventricular and outflow tract cushions (Fig. 13.1a). In chicken (Fig. 13.2a, b) and mouse embryos, the presence of the (sub)epicardium is less extensive compared to the turtle. In human embryos at Carnegie stages, 11–15 (3.6–7 mm), the surface of the heart is closely covered by the epicardial epithelium, whereas the inner curvature harbours an extensive epicardial cushion (Fig. 13.1b) comparable to the turtle.

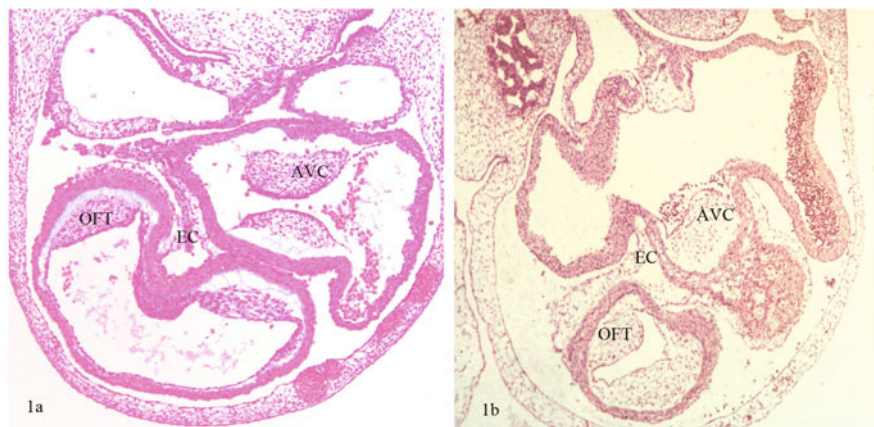


**Fig 13.1** (a, b) Sections of turtle (*Emys orbicularis*) (a) and human embryo (b) of comparable developmental stages showing the epicardial cushion (EC) in the inner curvature of the looping heart tube. AVC atrioventricular cushion, OFT outflow tract cushion

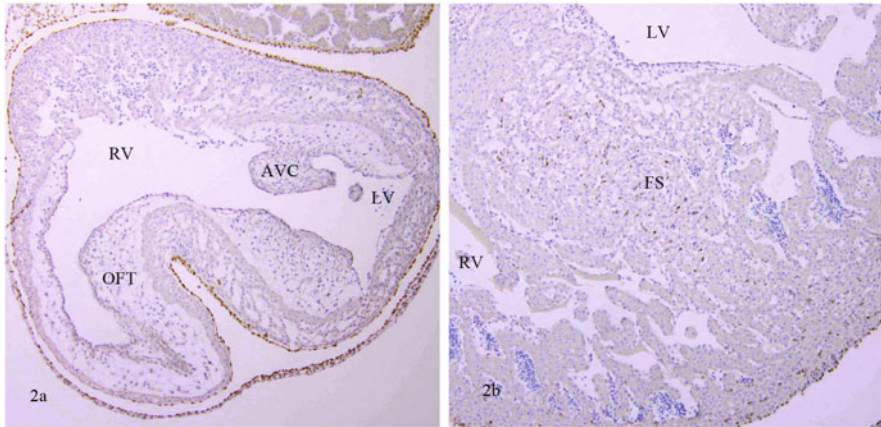


**Fig 13.2** (a) Chicken embryo stage 27 showing the start of the folding septum between OFT and AVC, stained for the Wilm's tumour antigen (WT1) marking the epicardium (*brown*). (b) Chicken embryo stage 31 with an elaborate folding septum (FS) showing dispersed EPDCs (*brown*) between the cardiomyocytes. *LV* left ventricle, *RV* right ventricle

### 13.4 The Epicardium in the Avian Heart

To investigate the fate of the epicardium during ballooning of the ventricles and subsequent folding of the septum, we constructed quail-chicken chimeras. An isochronic quail proepicardial organ (PEO) including a small piece of adjacent liver tissue to provide endothelial cells was transplanted into the pericardial cavity of HH15–17 chick embryos in an anterior position. Antibody staining revealed that quail EPDCs and endothelial cells were present in the anterior folding septum, but not in the dorsal inlet septum (Fig. 13.3a, b). The quail epicardial sheet dispersed into individual cells that became distributed between the cardiomyocytes in later stages, mostly in the core of the folding septum. In a second set of chimeras, the quail PEO was positioned more dorsally, providing for quail EPDCs and endothelial cells on the posterior ventricular surface, subsequently migrating into the inlet septum including the septal band, without crossing over to the anterior folding septum. This indicates the inlet septum as a separate component. Furthermore, an epicardial sheet, characteristic for the folding septum, was not encountered. As a consequence, expansion of the ventricles results in anterior folding of the ventricular wall, but not of the posterior wall, probably because of the physical constraints imposed by attachment of the heart to the dorsal body wall [10].

To study septum folding during ballooning of the ventricle, fluorescent DiI was tattooed (HH15–17) onto the ventral myocardial surface and embryos were sacrificed between HH22 and 33. DiI was applied on the surface of the future fold and the dye fragmented during further development into a left-sided part, incorporated into the left side of the folding septum and a right-sided part. This

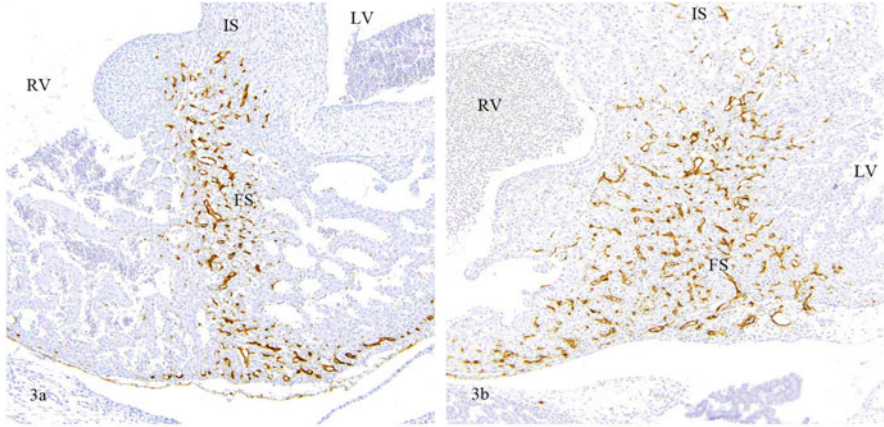


**Fig 13.3** (a, b) Quail-chicken chimeras from the anterior position. The folding septum (FS) harbours quail-derived endothelial cells stained with the QH1 antibody (*brown*), whereas the inlet septum (IS) is virtually negative

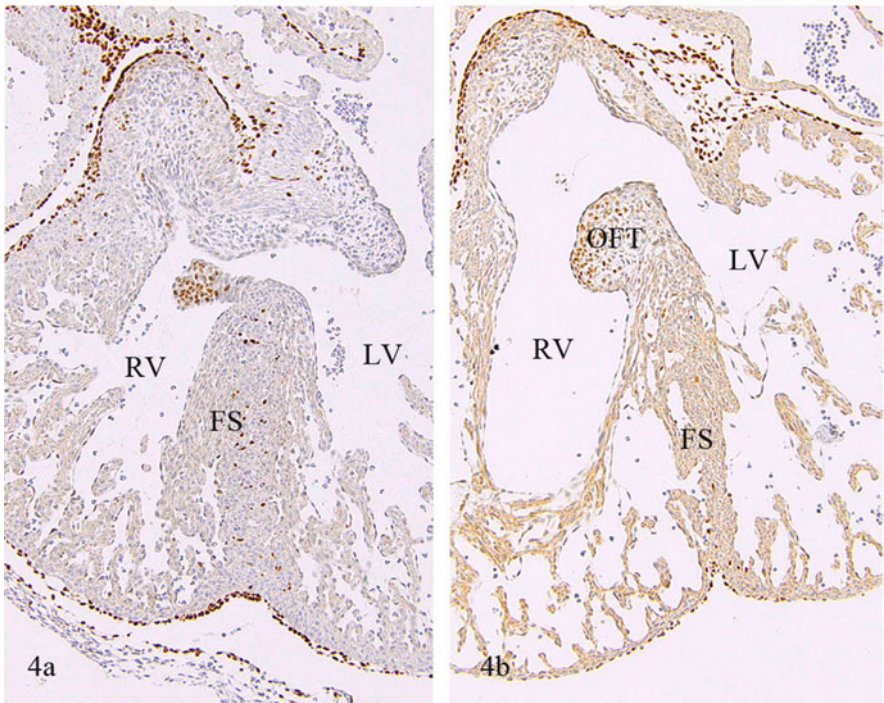
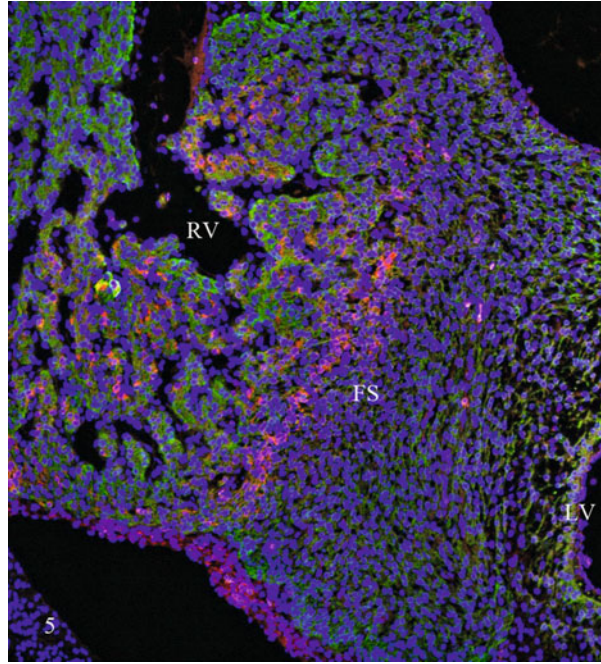


**Fig 13.4** Podoplanin wild type (a) and  $-/-$  mouse (b), embryonic day 12.5. Note the diminished number of epicardial cells and EPDCs (*brown* in this WT1 staining) and the thin folding septum in the mutant

**Fig 13.5** DiI-labelled chicken embryo stage 31 with a thin strip of the dye in the folding septum adjacent to the right ventricular surface



indicates a longitudinally directed morphogenetic expansion of the right ventricular wall compared to a transverse expansion of the left ventricle. At stage 31 the dye was completely embedded in the folding septum as a narrow fluorescent strip (Fig. 13.5) markedly close to the right ventricular face of the septum, indicative of a less elaborate right ventricular contribution to the septum [10].

### 13.5 Disturbance of the Epicardium

Deficient septation is known in several mouse mutants and we have analysed the podoplanin mutant mouse. Podoplanin has multiple roles in the maintenance of the epithelium and is expressed in the mesothelium of the body cavities including the epicardium. The knockout mouse presents with an underdeveloped PEO and abnormal epicardial covering resulting in only a few EPDCs [5]. The phenotype shows multiple malformations including an atrioventricular septum defect. At embryonic day 12.5, the myocardium and the folding septum are very thin, and the inlet septum is spongy. The diminutive septum is nearly devoid of EPDCs suggestive of an instructive role for these cells in septation (Fig. 13.4a, b).

---

### 13.6 Septum Components in Reptilian Hearts

The horizontal septum of developing reptiles is found in comparable stages and location, separating ventricular cavities and harbouring an epicardial sheet similar to the folding septum in mammals and birds. We prefer to address this structure as ‘folding septum’. The presence and extent of the vertical septum (homologous to inlet septum) differs among reptiles, being virtually absent in turtles and most non-crocodylian reptiles, but more prominent in varanids and pythonidae [11]. In the python myocardial apical trabeculations traverse the ventricle to partly separate the cavum pulmonale from the cavum arteriosum.

---

### 13.7 Tbx5 Expression Patterns

The transcription factor Tbx5 is implicated in full ventricular septation in mammals and is expressed strongly in the left part of the cardiac tube, with expression declining towards the right side [9]; we confirmed this expression pattern also in early stages of the copperhead rat snake, *Coelognathus*. Slightly later in the development, we show that embryonic turtle and python show expression of Tbx5 that declines at the folding septum, but not over the dorsal wall, where a sharp decline was found only near the outflow tract. In the chicken the *Tbx5* mRNA gradient identifies the right ventricle (weak expression) from the outflow tract (negative expression). Furthermore, a *Tbx5* decline is found at the folding septum showing only strong left-sided expression, whereas *Tbx5* expression is present on both sides of the inlet septum including the septal band. Thus, in the chicken the folding and inlet septa are differentially identified by Tbx5 gradients. In the mouse two Tbx5 gradients identify the inlet and folding septum. Protein expression is strongest in the trabeculations of the left ventricle, weaker in the right ventricular inlet including septal band and weakest to negative in the right ventricular outflow.

---

### 13.8 Discussion

All amniotes exhibit a folding (horizontal) septum, and here we showed the involvement of the epicardium in fusion of the two opposing myocardial walls. In mammals and birds, the folding septum forms the anterior part of the definitive septum. Reducing the size of the PEO leads to diminished or retarded covering of the myocardium and diminished production of EPDCs [4, 5, 12]. The latter can differentiate into smooth muscle cells of the coronary vessels and into perivascular and interstitial fibroblasts [13]. It is evident that mechanical or genetic interference with the epicardium or EPDCs not only disturbs coronary vascularisation but can also strongly influence cardiomyocyte differentiation and ventricular septation.

Different septal components [6, 7] have been identified in the completely septated hearts which have been the subject of continued debate also involving exploration of the position of central muscular ventricular septal defects and the

connection of the tricuspid valve tendinous cords related to either septal components. It was generally agreed that the septal band belonged to the primary septum being the anterior or, as we now refer to it, the folding component of the septum, but we demonstrated that it belongs to the posterior inlet septum. We newly identified the border between inlet and folding component using several criteria: (1) the atrioventricular cushions connect to the inlet component including the septal band; (2) the tip of the septal outflow tract cushion originates where the folding septum merges with the inlet septum; (3) quail cells derived from posterior PEO chimeras do not crossover from inlet septum including septal band to the folding septum, and vice versa in anterior chimeras, there is no crossover from folding to inlet septum; and (4) *Tbx5* expression, in contrast to earlier publications [9, 14], is strong on the left and right side of the posteriorly located inlet septum including the septal band, whereas only left-sided positivity is found at the anterior folding septum. From this we postulate that the avian and mammalian embryonic ventricle (homologous to the cavum dorsale of reptiles, which is the cavum arteriosum and venosum combined) give rise to both the left ventricle and the inlet of the right ventricle. This is an indication that the inlet septum originates in its entirety from the wall of the primitive ventricle, the cavum dorsale. In the right ventricle, the boundary of the inlet septum is provided by the septal band, which is not present in the left ventricle, leaving here the boundary between the inlet and folding septum less well determined. Our new model for separating the ventricles implicates more than one component and has consequences for understanding the development of central muscular ventricular septal defects. (Note: The development of the membranous and the outflow tract septum has not been specifically addressed in this study) Interestingly, elephants and some relatives including seacows show a very deep anterior interventricular sulcus [10]. The anatomy of the right ventricular septal band and the attachment of the tricuspid chordae tendineae suggest a diminished folding mechanism resulting in retention of an early embryonic state, also known as neoteny.

In conclusion, we have explored an evo-devo context for the hitherto overlooked role for the epicardium in septation and have clarified complex homologies in amniotes of the ventricular septum to understand clinical disorders of the heart in humans.

**Acknowledgements** B.J. is supported by the Danish Council for Independent Research | Natural Sciences and M.K.R. is supported by AgentschapNL, Smartmix SSM06010.

**Open Access** This chapter is distributed under the terms of the Creative Commons Attribution-Noncommercial 2.5 License (<http://creativecommons.org/licenses/by-nc/2.5/>) which permits any noncommercial use, distribution, and reproduction in any medium, provided the original author(s) and source are credited.

The images or other third party material in this chapter are included in the work's Creative Commons license, unless indicated otherwise in the credit line; if such material is not included in the work's Creative Commons license and the respective action is not permitted by statutory regulation, users will need to obtain permission from the license holder to duplicate, adapt or reproduce the material.

## References

1. Holmes EB. A reconsideration of the phylogeny of the tetrapod heart. *J Morphol.* 1975;147:209–28.
2. Jacobs JP, et al. Congenital heart surgery nomenclature and database project: atrial septal defect. *Ann Thorac Surg.* 2000;69:S18–24.
3. Gittenberger-de Groot AC, et al. Epicardium-derived cells contribute a novel population to the myocardial wall and the atrioventricular cushions. *Circ Res.* 1998;82:1043–52.
4. Lie-Venema H, et al. Origin, fate, and function of epicardium-derived cells (EPDCs) in normal and abnormal cardiac development. *Sci World J.* 2007;7:1777–98.
5. Mahtab EAF, et al. Cardiac malformations and myocardial abnormalities in podoplanin knockout mouse embryos: correlation with abnormal epicardial development. *Dev Dyn.* 2008;237:847–57. doi:[10.1002/dvdy.21463](https://doi.org/10.1002/dvdy.21463).
6. Wenink ACG. Embryology of the ventricular septum. Separate origin of its components. *Virchows Arch.* 1981;390:71–9.
7. van Mierop LH, Kutsche LM. Development of the ventricular septum of the heart. *Heart Vessels.* 1985;1:114–9.
8. Darnell DK, et al. Dynamic labeling techniques for fate mapping, testing cell commitment, and following living cells in avian embryos. *Methods Mol Biol.* 2000;135:305–21.
9. Koshiha-Takeuchi K, et al. Reptilian heart development and the molecular basis of cardiac chamber evolution. *Nature.* 2009;461:95–8. doi:[10.1038/nature08324](https://doi.org/10.1038/nature08324).
10. Poelmann RE et al. Evolution and development of ventricular septation in the amniote heart. *PLoS ONE* 2014;9(9):e106569. doi:[10.1371/journal.pone.0106569](https://doi.org/10.1371/journal.pone.0106569)
11. Jensen B, et al. Structure and function of the hearts of lizards and snakes. *Biol Rev Camb Philos Soc.* 2014;89:302–36.
12. Gittenberger-de Groot AC, et al. Epicardial outgrowth inhibition leads to compensatory mesothelial outflow tract collar and abnormal cardiac septation and coronary formation. *Circ Res.* 2000;87:969–71.
13. Gittenberger-de-Groot AC, et al. The arterial and cardiac epicardium in development, disease and repair. *Differentiation.* 2012;84:41–53. doi:[10.1016/j.diff.2012.05.002](https://doi.org/10.1016/j.diff.2012.05.002).
14. Greulich F, Rudat C, Kispert A. Mechanisms of T-box function in the developing heart. *Cardiovasc Res.* 2011;91:212–22. doi:[10.1093/cvr/cvr112](https://doi.org/10.1093/cvr/cvr112).

Hajime Fukui, Shigetomo Fukuhara, and Naoki Mochizuki

## Keywords

Zebra fish • Sphingosine-1-phosphate • *Cardia bifida* • Endoderm

During embryogenesis, zebra fish cardiac precursor cells (CPCs) originating from anterior lateral plate mesoderm migrate toward the midline between the endoderm and the yolk syncytial layer (YSL) to form cardiac tube. The endoderm functions as a foothold for CPCs as evidenced by the endodermal mutants (*cas/sox32*, *sox17*, *oep*, *faul/gata5*, and *bon*) showing two hearts (*cardia bifida*) [1]. Furthermore, mutant zebra fish (*toh*) lacking sphingosine-1-phosphate (S1P) transporter which is expressed in the YSL show two hearts [2], indicating the essential role for S1P-mediated signal in cardiac development. This is also supported by a S1p2 receptor mutant (*mil*) which exhibits two hearts [3]. However, it is still unclear how S1P released from YSL regulates CPC migration.

S1p2 is expressed in the endoderm. Thus, we assume that S1P released from the YSL might activate S1p2 expressed in the endoderm, thereby regulating CPC migration. One possibility is that S1p2-mediated signal controls the endoderm formation as a foothold for CPCs. Another possibility is that endodermal cells activated by S1p2 might secrete the chemokines which accelerate CPC migration or secrete the extracellular matrix proteins for guiding CPC movement.

To test these possibilities, we need to delineate the downstream signaling of S1p2. Recently,  $G\alpha_{13}$  is reported to inhibit Hippo-mediator Lats1/2 kinase through a RhoGEF/Rho/Rho-kinase signaling [4, 5]. We demonstrate that the inhibition of Hippo signaling in the endoderm by activated S1p2 is essential for endodermal cell

---

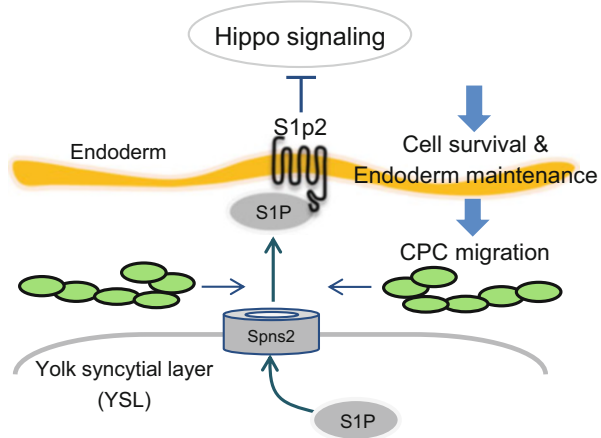
H. Fukui • S. Fukuhara • N. Mochizuki (✉)

Department of Cell Biology, National Cerebral and Cardiovascular Center Research Institute, Fujishirodai 5-7-1, Suita, Osaka 565-8565, Japan

e-mail: [nmochizu@ncvc.go.jp](mailto:nmochizu@ncvc.go.jp)



**Fig. 14.1** A model of S1P-S1p2 signaling regulated CPC migration. S1P secreted from the yolk activates S1p2 in the endoderm. Hippo signaling acts downstream of S1P-S1p2 signaling and maintains the endoderm to act as scaffolds for CPC migration



survival and that the endoderm maintained by S1P signaling indeed becomes the foothold for CPC migration (Fig. 14.1).

**Open Access** This chapter is distributed under the terms of the Creative Commons Attribution-Noncommercial 2.5 License (<http://creativecommons.org/licenses/by-nc/2.5/>) which permits any noncommercial use, distribution, and reproduction in any medium, provided the original author(s) and source are credited.

The images or other third party material in this chapter are included in the work's Creative Commons license, unless indicated otherwise in the credit line; if such material is not included in the work's Creative Commons license and the respective action is not permitted by statutory regulation, users will need to obtain permission from the license holder to duplicate, adapt or reproduce the material.

## References

1. Kikuchi Y, et al. *casanova* encodes a novel Sox-related protein necessary and sufficient for early endoderm formation in zebrafish. *Genes Dev.* 2001;15(12):1493–505.
2. Kawahara A, et al. The sphingolipid transporter *spns2* functions in migration of zebrafish myocardial precursors. *Science.* 2009;323(5913):524–7.
3. Kupperman E, et al. A sphingosine-1-phosphate receptor regulates cell migration during vertebrate heart development. *Nature.* 2000;406:192–5.
4. Ye D, Lin F. S1pr2/Gα<sub>13</sub> signaling controls myocardial migration by regulating endoderm convergence. *Development.* 2013;140:789–99.
5. Yu FX, et al. Regulation of the Hippo-YAP pathway by G-protein-coupled receptor signaling. *Cell.* 2012;150(4):780–91.

---

# Myogenic Progenitor Cell Differentiation Is Dependent on Modulation of Mitochondrial Biogenesis through Autophagy 15

Yoshimi Hiraumi, Chengqun Huang, Allen M. Andres, Ying Xiong, Jennifer Ramil, and Roberta A. Gottlieb

---

## Abstract

Over the last decade, stem/progenitor cell therapy has emerged as an innovative approach to promote cardiac repair and regeneration. However, the therapeutic prospects of are currently limited by inadequate means to regulate cell proliferation, homing, engraftment, and differentiation. Autophagy, a lysosome-mediated degradation pathway for recycling organelles and protein aggregates, is recognized as important for facilitating cell differentiation. Studies have shown that induced pluripotent stem cells (iPCs), which exhibit a predominantly glycolytic metabolism, shift toward oxidative mitochondrial metabolism as a prerequisite for the formation of sarcomeres and differentiation into cardiomyocytes. C2C12 myoblasts are a mouse-derived myogenic progenitor cell line which can be induced to differentiate into myotubes. We hypothesize that autophagy is essential in coordinating transcription factor activity and metabolic reprogramming of mitochondria to support myocyte differentiation.

---

## Keywords

Autophagy • Stem cell • Differentiation

C2C12 myoblasts were cultured in DMEM (10 % FBS) and induced to differentiate into myotubes with DMEM (2 % horse serum) for 6 days. To disrupt autophagy, cells were (1) transfected with 50 nM Atg5 siRNA for 8 h twice over a 48 h period

---

Y. Hiraumi (✉)

Department of Pediatrics Cardiology, Hyogo Amagasaki Prefecture Hospital, Higashidaimotsu-cyo 1-1-1, Amagasaki, Hyogo 660-0828, Japan  
e-mail: [hirahira@kuhp.kyoto-u.ac.jp](mailto:hirahira@kuhp.kyoto-u.ac.jp)

C. Huang • A.M. Andres • Y. Xiong • J. Ramil • R.A. Gottlieb  
Donald P. Shiley BioScience Center, San Diego State University, 5500 Campanile Drive, San Diego, CA 92182-4650, USA

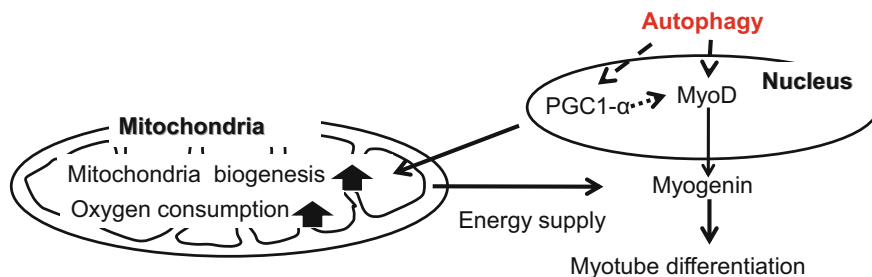


**Fig. 15.1** Proposed mechanism for the role of autophagy in C2C12 cell differentiation. Upregulation of PGC1 $\alpha$ , MyoD, and myogenin is a hallmark of cell differentiation. Transcription factor regulation by autophagy may affect mitochondrial turnover required for C2C12 cell differentiation. Autophagy is essential for coordinating transcriptional regulation and mitochondrial dynamics to support the progression of cell differentiation

or (2) treated with 10 nM bafilomycin A1 or vehicle control for a 3 h/day for the first 3 days of differentiation. GFP-LC3 adenovirus was employed to visualize autophagy. Western blot and real-time qPCR were used to examine proteins and transcripts of interest. We observed increased LC3-II levels and GFP-LC3 puncta during the differentiation of C2C12 cells, suggesting the involvement of autophagy in this process. Transient inhibition of autophagy during the early stages of differentiation with either Atg5 siRNA or bafilomycin A1 interfered with myotube formation and attenuated the upregulation of myogenic transcription factors MyoD and myogenin. Differentiation was accompanied by an increase in PGC1 $\alpha$  mRNA, mitochondrial mass, and oxygen consumption, all of which were blocked by disruption of autophagy. Autophagy coordinates transcription factor expression and mitochondrial turnover essential for cell differentiation (Fig. 15.1).

**Open Access** This chapter is distributed under the terms of the Creative Commons Attribution-Noncommercial 2.5 License (<http://creativecommons.org/licenses/by-nc/2.5/>) which permits any noncommercial use, distribution, and reproduction in any medium, provided the original author(s) and source are credited.

The images or other third party material in this chapter are included in the work's Creative Commons license, unless indicated otherwise in the credit line; if such material is not included in the work's Creative Commons license and the respective action is not permitted by statutory regulation, users will need to obtain permission from the license holder to duplicate, adapt or reproduce the material.

Kazuhiro Maeda, Sachiko Miyagawa-Tomita, and Toshio Nakanishi

## Keywords

Thyroid • Thyroid hormone • Thyroid hormone receptor • Heart • Chick embryo

Congenital hypothyroidism (CH) is one of the most common diseases of the endocrine system among newborns. Infants with CH have been reported to have a high frequency of congenital cardiovascular malformations (CM), such as ventricular and atrial septal defects [1]. Some studies have demonstrated that these cases were due to gene mutations and neural crest abnormality. Infants with CH and CM have been shown to have significantly lower T<sub>4</sub> levels than those with isolated CH. However, the role of thyroid hormone in the developing heart has not been reported. In this study, we show the thyroid anlage in chick embryos by immunohistochemistry and follow the expression of thyroid hormone receptor during heart development.

1. The thyroid anlage appeared close to the aortic sac at H/H 14 of chick embryos, as determined by immunohistochemistry (Fig. 16.1a).
2. Avians have access to thyroid hormone long before the embryonic thyroid gland starts to secrete hormones due to the hormone deposition in the yolk and egg white [2].
3. We found that the expression of thyroid hormone receptors during embryonic heart development was earlier than that reported previously published study using RT-PCR (Fig. 16.1b) [3].

---

K. Maeda • T. Nakanishi

Department of Pediatric Cardiology, Tokyo Women's Medical University, 8-1 Kawada-cho, Shinjuku-ku, Tokyo 162-8666, Japan

S. Miyagawa-Tomita (✉)

Department of Pediatric Cardiology, Division of Cardiovascular Development and Differentiation, Medical Research Institute, Tokyo Women's Medical University, Tokyo, Japan

e-mail: [ptomita@hij.twmu.ac.jp](mailto:ptomita@hij.twmu.ac.jp)

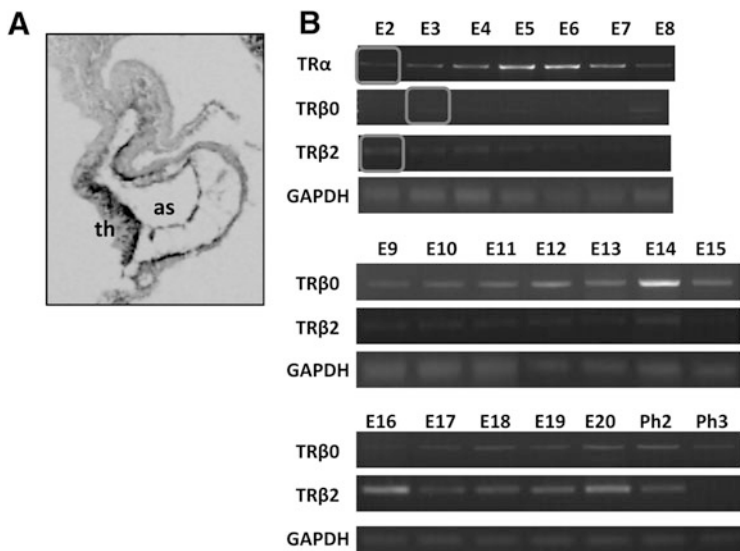


**Fig. 16.1** (a) The thyroid anlage appeared close to the aortic sac at H/H 14. *as* aortic sac, *th* thyroid anlage. (b) The expression of thyroid hormone receptors in the developing chick heart. TR $\alpha$  and TR $\beta$ 2 were expressed beginning on E2, and TR $\beta$ 0 was expressed beginning on E3 (circled). *E* embryonic day, *Ph* post hatching day

These results suggest that thyroid hormone may contribute to the development of the heart.

**Open Access** This chapter is distributed under the terms of the Creative Commons Attribution-Noncommercial 2.5 License (<http://creativecommons.org/licenses/by-nc/2.5/>) which permits any noncommercial use, distribution, and reproduction in any medium, provided the original author(s) and source are credited.

The images or other third party material in this chapter are included in the work's Creative Commons license, unless indicated otherwise in the credit line; if such material is not included in the work's Creative Commons license and the respective action is not permitted by statutory regulation, users will need to obtain permission from the license holder to duplicate, adapt or reproduce the material.

## References

- Olivieri A, Stazi MA, Mastroiacovo P, et al. A population-based study on the frequency of additional congenital malformations in infants with congenital hypothyroidism: data from the Italian Registry for Congenital Hypothyroidism (1991–1998). *J Clin Endocrinol Metab.* 2002;87:557–62.
- Prati M, Calvo R, Morreale G, Morreale de Escobar G. L-thyroxine and 3,5,3'-triiodothyronine concentrations in the chicken egg and in the embryo before and after the onset of thyroid function. *Endocrinology.* 1992;130:2651–9.
- Forrest D, Sjöberg M, Vennström B. Contrasting developmental and tissue-specific expression of alpha and beta thyroid hormone receptor genes. *EMBO J.* 1990;9:1519–28.